Climate Hazards and Resilience in the Global Car Industry*

Juanma Castro-Vincenzi

Harvard University

February 1, 2024

Abstract

Climate change will increase the frequency and severity of natural disasters. This paper examines the effects of such increases on the spatial organization of firms. Using data on the global car industry and an event-study design, I document that nearby floods significantly reduce assembly plant production, with partial reallocation to unaffected plants within the firm. I develop a novel, quantitative, multiregion model in which firms choose their plant locations and capacities to maximize expected profits amidst weather disruption risk. The model captures firms' incentives to diversify capacity across locations and hedge against potential local disruptions. I estimate the model for the automotive industry and use it to compute plant location and capacity choices under different probabilities of weather disruptions according to possible climate change scenarios. With heightened risks, firms build additional, smaller plants with larger spare capacities. This spatial reorganization entails productivity losses, resulting in higher consumer prices.

JEL Classifications: F12, F18, F23, L23, Q54, Q56

*I am grateful to Gene Grossman, Eduardo Morales, Ezra Oberfield, and Esteban Rossi-Hansberg for their guidance, and support. I thank Allan Hsiao, Ishan Nath, Stephen Redding, Catherine Thomas, and Jose P. Vásquez for detailed discussions and comments. This paper benefited from conversations with Clare Balboni, Leah Boustan, Elaine Buckberg, Paula Bustos, Lorenzo Caliendo, Pablo Fajgelbaum, Stefania Garetto, Cecile Gaubert, Matthew Kahn, Benny Kleinman, Michal Kolesár, Hugo Lhuillier, Isabela Manelici, Joan Monras, Jacopo Ponticelli, Andrés Rodríguez-Clare, Richard Rogerson, Alejandro Sabal, Joseph Shapiro, Felix Tintelnot, and Daniel Trefler, and from the comments of numerous seminar and conference participants. This research was supported by the International Economics Section (IES) at Princeton University. All errors are my own. Email: jcastrovincenzi@fas.harvard.edu.

1 Introduction

This paper studies how the likelihood of extreme weather events shapes the spatial organization of firms. With the Intergovernmental Panel on Climate Change's Sixth Assessment Report (IPCC 2021a) predicting an increase in the frequency and severity of weather-related natural disasters due to global warming, it becomes essential to comprehend how firms can adapt to these changing conditions. Understanding the potential adaptation costs, as how firm-level adaptation can buffer the impact of climate change on firms' profits and consumer welfare, is particularly relevant.

As responses to the rise in the frequency of weather disasters caused by a changing climate, this paper explores two potential mechanisms of endogenous firm-level adaptation. First, firms can modify their production sites' location and capacity. Second, firms with multiple production sites can exploit the flexibility built into their plant structure to reallocate production from affected to unaffected plants.

These adaptation mechanisms could entail high costs for firms and consumers. When firms reallocate production capacity across locations in response to climate hazards, they shift production from more ex-ante productive places to less productive ones. As a result, consumers experience higher prices and reduced variety, decreasing their surplus. Creating a resilient production structure is also costly. Setting up multiple plants to hedge against adverse shocks requires a sizable capital investment, and exploiting the flexibility of a multiplant scheme requires holding sites that operate with spare capacity.

I examine these specific adaptation margins in the global car industry.[1] This industry provides an ideal setting for studying this question, comprising multinational, multiplant firms producing tradeable goods in physical sites susceptible to weather disasters. To this end, I leverage a rich global dataset that links the production location at the plant level with sales of individual car models.

Numerous car industry examples highlight these adaptation mechanisms. One notable instance involves a Honda plant in Celaya, Mexico, that had to suspend operations for nearly three months when torrential precipitation caused the local river to flood. While Honda had prepared by setting up another plant in El Salto, about 160 kilometers away, it could only partially compensate for the production loss due to its smaller capacity.[2]

[1] For example, in their 2021 Carbon Disclosure Project Report (CDP-BMW 2021), BMW states that flexible production structures allow them to respond to business interruptions caused by physical climate drivers, e.g., if the X3 production in Spartanburg is shut down, they can shift volumes to Rosslyn or Shenyang.

[2] In Appendix A.1, I present a collection of news headlines about extreme weather events that have caused significant disruptions to car production. In Figure A.1 in the Appendix, I show graphical evidence

In the first part of the paper, I present evidence of severe floods' disruptive consequences on car production. These floods result from various meteorological and hydrological phenomena, such as extreme rainfall, rapid snowmelt, tropical cyclones, and coastal storms, likely intensified by climate change.[3] Floods affect car production through direct damage to facilities, transportation challenges for goods, inputs, and labor, and indirect impacts on infrastructure and local supply chains.[4] The timing of these events is exogenous to local industry characteristics, and detailed historical flood data are available.

Using an event-study design, I document that a severe flood close to a car assembly site causes a long-run decline in a plant's production of around 30%. Multiplant firms reallocate some production to their unaffected sites. By leveraging information on the production of narrowly defined car models, I estimate that when a flood affects a plant, production in other plants that produce at least one of the same models rises by 46%. However, firms are able to offset only part of the decline by ramping up production at their other plants.

I develop a multiregion model of optimal plant location to understand how firms adapt to the increasing likelihood of floods and assess the costs of these adaptation mechanisms. In the model, firms are potentially multinational and can operate multiple plants as platforms to serve different markets, as in Helpman et al. (2004) and Tintelnot (2017). Firms choose their production plants' location and capacity to maximize expected profits. They face uncertainty about the exact productivity of each plant when making an irreversible investment in plant capacity. After capacity is installed, productivity shocks, in the form of adverse weather events, are realized, and firms choose the optimal production flows from each plant to each market, conditional on their sunk plant location and capacity choices.

In deciding their plant configuration, firms face a tradeoff between proximity, cost minimization, and resilience. Trade costs provide incentives to set up plants close to large markets. Locating plants close to customers might sacrifice setting up plants in locations that minimize production costs. These two potentially conflicting incentives interact with a third margin: production resilience. Since adverse productivity shocks occur with a certain probability, firms have additional incentives to invest in capacity in multiple locations to hedge against production disruptions in one of their plants.

of the flood, its impact on Honda's production in the region, and the geographical location of both plants.

[3] See, e.g, IPCC 2021a, Hirabayashi et al. 2021, Bates et al. 2021, Li et al. 2022, and World Meteorological Organization (2022).

[4] Ellison and Glaeser (1997) show that final assembly and car parts are among the most colocated industry pairs in the United States. Klier and Rubenstein (2008) indicate that for the assembly plants in their sample, 5% of independent suppliers are located within 60 miles. For powertrains and transmissions, Head et al. (2024) note that 40% of powertrains and 20% of transmissions are sourced within 100km of the assembly plant.

The resilience motive naturally arises because firms can adjust production in response to realized productivity shocks, allowing them to shift production from disrupted to undisrupted plants. However, the option to switch production across plants is constrained by their initial investments in capacity. Ex-ante, firms have incentives to hold additional capacity in their chosen locations to hedge against potential plant disruptions.

Plant location and capacity choices are interdependent across locations because plants can be export platforms. These decisions must be taken jointly, which is challenging if the number of potential locations is significant, as in the global car industry. The problem is further complicated because it involves optimization under uncertainty over a large set of states of the world. Rather than devolving into a combinatorial discrete choice problem, in the model, the optimal plant capacity choices are the solution to a convex optimization problem for which efficient numerical algorithms exist.

The model delivers quantitative predictions about the geography of global production, namely, where plants are located, how large these plants are, where cars are produced, and the flows of vehicles between production locations and markets. I estimate the model by matching the current geographic distribution of car production. I leverage the structure of the model to estimate demand parameters and trade costs, and simulation-based methods to estimate the determinants of productivity and capacity costs for each location.

The main goal of the quantitative model is to evaluate how firms will choose their production locations as the probability of weather disasters increases. I draw upon projections from the CMIP6 climate models to inform these probability increases in specific regions. Precisely, I measure the likelihood of these adverse weather events as the probabilities of historical 10- and 100-year five-day precipitation events, a proxy for floods, happening in a given location under different Shared Socioeconomic Pathways (SSPs), which capture alternative possible future greenhouse gases emission trajectories, for the period 2035–2064.

Changes in the probabilities of extreme weather events are heterogeneous across space. For instance, in SSP5-8.5, the worst-case emissions scenario considered by the IPCC, the probability of a 100-year five-day precipitation event, which historically is 1% in any given year, is expected to increase in Tennessee to 2.2%, in Michigan to 2.3%, and in Tokyo to 1.4%. By contrast, the probability of such an event in Tangier, Morocco, decreases to 0.8%. On average, in this climate change scenario, 10-year extreme precipitation events and 100-year extreme precipitation events become 1.46 and 1.89 times more likely, respectively.

In my main counterfactual exercise, I change probabilities from the current flood risk landscape to the probabilities projected by climate change models in the SSP5-8.5 scenario and recompute plant locations and capacities for each firm. With heightened risks, firms

build additional, smaller plants. The average firm increases its number of plants by 3.6%, but the average capacity per plant decreases by 7.1%. Firms shrink considerably; on average, production capacity declines by 4.8% and profits by 4.0%. Firms operate with more spare capacity, holding 7.0% of their total capacity for hedging purposes.

These findings reveal that firms can adapt to an increase in the probability of adverse weather events by investing in more plants, thereby reducing their exposure to local disruptions. Also, firms hold more spare capacity in their plants to have the option to reallocate production after adverse shocks. This reorganization is costly, as firms shrink while bearing the costs of disproportionately large capacity choices to hedge against disruptions.

Geographically, firms increase production and capacity in places close to large markets with relatively smaller probabilities of extreme precipitation events, such as Central Mexico, the Western United States, Northern Africa, Turkey, Southern India, and the South of Europe. On the other hand, there is a decrease in production in England, the US Midwest, Western India, and Northeastern France. With this reallocation, average productivity declines by 7.1%, and consumer prices increase by 2.6%. Although almost all countries experience increased consumer prices, the incidence is heterogeneous.

Regarding how effective this adaptation is at reducing the losses due to climate change, the average profit decline is 4.1% when firms reoptimize their plant configuration choices. In contrast, this decline would be 5.3% if firms do not adapt. Leveraging these adaptation channels, car firms can avoid approximately 20% of the prospective losses from climate change. However, firm-level adaptation reduces consumer surplus. For consumers, the reallocation of plants across space is an aggregate shock as all varieties become more expensive due to the losses in productivity and capacity. When firms do not adapt to climate change, consumer price indices increase, on average, by 1.0% as disruptions to individual firms are not very costly for consumers in industries with many varieties. Consumers can adapt to idiosyncratic increases in the price of one variety by substituting it for others.

This paper relates to several strands of the literature. First, it is closely related to the literature that studies the impact of climate change and weather disasters on the distribution of economic activity across and within cities, regions, and countries (e.g., Desmet et al. 2021, Balboni 2021, Nath 2022, Jia et al. 2022, Cruz and Rossi-Hansberg 2023, Hsiao 2023, and Bilal and Rossi-Hansberg 2023). This paper contributes novel insights by empirically and theoretically analyzing mechanisms of endogenous potential adaptation that firms can use to lessen the impact of extreme weather events caused by a changing climate. Additionally, it is closely related to Indaco et al. (2020), Pankratz and Schiller (2021), Gu and Hale (2022), Balboni et al. (2023) and Castro-Vincenzi et al. (2024a), that explore the effect of

weather disasters on firms' employment, supplier choice, FDI and production networks.

Second, this paper adds to the literature on the location of multinationals. Several papers study multinational production, quantitatively or theoretically, such as Helpman et al. (2004), Ramondo and Rodríguez-Clare (2013), Ramondo et al. (2013), Tintelnot (2017), Arkolakis et al. (2018), Head and Mayer (2019) and Arkolakis et al. (2023). This paper studies the joint problem of location and capacity choice that had not been introduced in quantitative multinational models before. Including capacity constraints allows me to provide a general framework for analyzing how changes in the probability distribution of demand or supply shocks affect firms' optimal plant location and how these shocks propagate within their plant network.[5]

The computational approach I introduce is novel to the quantitative plant location literature. The two dominant approaches to studying these problems consist of either choosing for each market, the least cost supplier, abstracting from fixed costs, making sourcing decisions independent of each other (e.g., Ramondo et al. 2013, Ramondo 2014 or Arkolakis et al. 2018), or including fixed costs, allowing for interdependencies across choices, but creating a high-dimensional, nonconvex problem (e.g., Tintelnot 2017, Arkolakis et al. 2023).[6] Instead, I formulate the firm's plant location and capacity choice problem as a convex optimization that allows for interdependencies while preserving computational tractability.

Third, this paper is related to the literature that studies supply chain resilience and disruptions. Jiang et al. (2021), Kopytov et al. (2023), Grossman et al. (2023a) and Grossman et al. (2023b) analyze, theoretically, the incentives for investment in resilience and optimal policy when firms face potential supply chain disruptions. These supply chain disruptions are quantitatively significant, as shown by Barrot and Sauvagnat (2016), Boehm et al. (2019), and Carvalho et al. (2020), all of whom leverage natural disasters to study the role of firm-level linkages in propagating input disruptions. I contribute to this literature by proposing a quantitative framework with investment in resilience to disruptions through plant organization in the face of an increase in risk.

The rest of the paper is structured as follows. In Section 2, I describe the data and

[5]This paper also builds on the theoretical literature pioneered by Pindyck (1988), Pindyck (1993) and Dixit and Pindyck (1994) that characterizes the problem of a firm making an irreversible capacity investment under uncertainty about output or input prices. For multinationals, Rob and Vettas (2003) study, theoretically, the tradeoff between exporting or creating productive capacity via FDI to serve a foreign market when demand is uncertain.

[6]See Antràs et al. (2017), Antràs et al. (2022), Alfaro-Ureña et al. (2024), and Castro-Vincenzi et al. (2024b) for examples of papers in international trade that solve combinatorial problems with interdependencies by leveraging properties of payoff functions.

document the impact of large floods on car production using an event-study design. In Section 3, I present a theoretical model of plant location with capacity constraints and an efficient solution strategy. Section 4 describes the estimation strategy for the structural model. Section 5 contains different climate change counterfactuals. Section 6 concludes.

2 Empirical Evidence

In this section, I estimate the effect of severe floods on car plants' production using detailed global plant-level production data for the automotive industry between 2000-2019 and data on historical floods since 1985.

2.1 Data

I use a dataset compiled by IHS Markit of new car registrations that reports quarterly flows of individual car models by plant of assembly and country of sale. The dataset covers the period 2000-2019 and contains information for 354 car brands, 77 countries of sale, and 1105 production plants in 54 countries. In a given quarter, the average firm has three active plants, the median number of plants per firm is 2, the $90th$ percentile is 7, and the maximum is 18. Different versions of this data have been used in previous literature, e.g., in Coşar et al. (2016) and Head and Mayer (2019).

I use the geographical coordinates of each plant's location to map them to Global Administrative Unit Layers (GAUL), which are a set of administrative units with global coverage that are consistent across years and borders, created by the Food and Agriculture Organization (FAO).[7] These administrative units have two spatial levels, GAUL1, which corresponds to the first layer in the hierarchy within a country administrative organization, e.g. states in the United States, and GAUL2, which is the second level, e.g. counties in the United States. Plants are located in 301 GAUL1 units and 554 GAUL2 units.

I obtain information about historical floods from the Dartmouth Flood Observatory (DFO), which uses different sources, such as news, governmental statements, satellite imagery, and remote sensing, to create the Global Archive of Large Flood Events. For each flooding event, the database collects information about the start and end dates of the event, the causes of the flood, an estimate of the geographical location, and a measure of severity. This archive starts in 1985.

In Figure 1, I show a map with the global distribution of assembly plants and the location of the floods in the dataset. The map shows that car plants are mostly located in

[7] More information about the Global Administrative Unit Layers of the FAO can be found in the following website https://data.apps.fao.org/map/catalog/static/api/records/9c35ba10-5649-41c8-bdfc-eb78e9e65654.

Figure 1: The Location of Car Production Plants and Floods

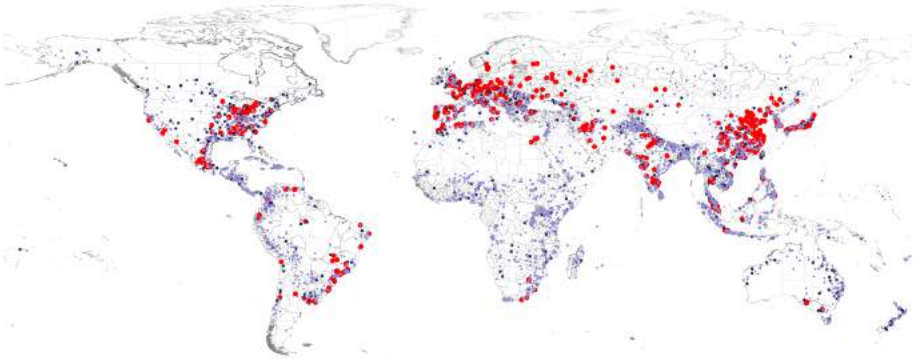

Notes: In this map, the red dots correspond to the location of a plant in the car production dataset. The dark blue dots correspond to centroids of 100-year floods that have taken place since 2000. Light blue dots correspond to 10-year floods. The administrative borders in gray correspond to GAUL1 units.

the Midwest of the United States, Western Europe, Eastern China, Japan, and Southeast Asia. It also reveals that, currently, car plants are located in places that have experienced floods.

Flooding events are rare, affecting plants in very few periods. Plants are affected by floods occurring at most 100km away in only 2.4% of the quarters—however, 77% of the plants in the sample experience a flood between 2000 and 2019. On average, 1.9 floods occur less than 100km from a plant.[8] By flood severity, floods with a recurrence interval of 10 years are more frequent than 100-year floods. 70% of plants experienced a 10-year flood close to them, but only 25% of the plants are affected by 100-year events.

For most of the empirical analysis, the unit of observation is the production plant and the main outcome is the log of the quantity of cars produced in an assembly plant in a quarter.[9] I define the treatment as the occurrence of a flooding event with a centroid 100 kilometers or less away from a car assembly plant, although the results are robust to different distance thresholds. In all the specifications, standard errors are clustered at the GAUL-1 level to capture potential correlation in the error terms across plants located in the same administrative unit and serial correlation over time.

2.2 Estimation Strategy

To estimate the effect of severe floods on car production, I use the estimator suggested in de Chaisemartin and D'Haultfoeuille (2022a). This is a differences-in-differences estimator

[8] From 2000 to 2019, 20% of plants were within 25km of at least one flood, and 40% within 50km.

[9] It is worth noting that I infer plant production in a quarter from data on registration. According to IHS, the average time between production and registration is around a month for domestic transactions to three quarters for international transactions. However, there is variation in lead times depending on demand and supply conditions.

of contemporaneous and dynamic treatment effects robust to heterogeneity that allows for the treatment to vary over time. It is given by,

$$DID_{i\ell} = Y_{i,F_i+\ell} - Y_{i,F_i-1} - \sum_{i':F_{i'}>F_i+\ell} \frac{1}{\sum_{i':F'_i>F_i+\ell} 1} \left(Y_{i',F_i+\ell} - Y_{i',F_i-1}\right),$$

which aggregates into

$$DID_{+,\ell} = \sum_{i:F_i+\ell\leqslant T} \frac{DID_{i\ell}}{N^1_\ell}, \tag{1}$$

where $Y_{i,F_i+\ell}$ corresponds to the outcome of interest for observation i at moment ℓ periods after plant i received the treatment for the first time in period F_i. N^1_ℓ are the number of plants, reaching ℓ periods after their first extreme flood, before or at the end of the sample period T. The estimator compares the value of the outcome for units that were treated ℓ periods ago with units not-yet treated ℓ periods after each unit's first treatment. The first difference compares the outcome ℓ periods after the plant was treated for the first time with the outcome the period before the unit was treated, and the second difference compares this long difference with the average difference for not-yet treated units by period $F_i + \ell$.

2.3 The Impact of Weather-Related Disasters on Car Production

I start by estimating the effect of the occurrence of a flood close to a plant on the number of cars produced.[10] In Figure 2a, I show the estimates of Equation 1 for the periods between the moment of the first flood up until 40 quarters afterward. The effect of floods on plant production is persistent and negative, stabilizing around 20 quarters after the first treatment. I compute the long-run effect by averaging the point estimates for 20 to 40 quarters after the unit was treated for the first time. This figure shows that the long-run effect caused by a flood on car production is a reduction in the number of cars produced of about 0.34 log points relative to production in plants that have not been yet treated.

In Figures 2b and 2c, I estimate event studies corresponding to floods with a 100-year recurrence interval and floods with at least a 10-year recurrence interval, but less than 100-year. As expected, the effect of the most severe floods, the 100-year floods, is sizable and negative. The long-run effect of the occurrence of a 100-year flood close to a plant indicates that the most severe floods in the sample reduce car production in 0.69 log points. For the less severe floods, the long-run effect corresponds to a decrease of 0.28 log points.

[10]The sample used to estimate the total impact of floods on car production comprises assembly plants that produce 50 units or more during all quarters between 2000-2019 and did not experience any flooding events in the 28 quarters before the first period in the sample (2000Q1) to avoid mislabeling plants that had already experienced a treatment before the sample as being untreated.

Figure 2: The Impact of Severe Floods on Car Production

(a) All Floods (b) 100-Year Floods (c) 10-Year Floods

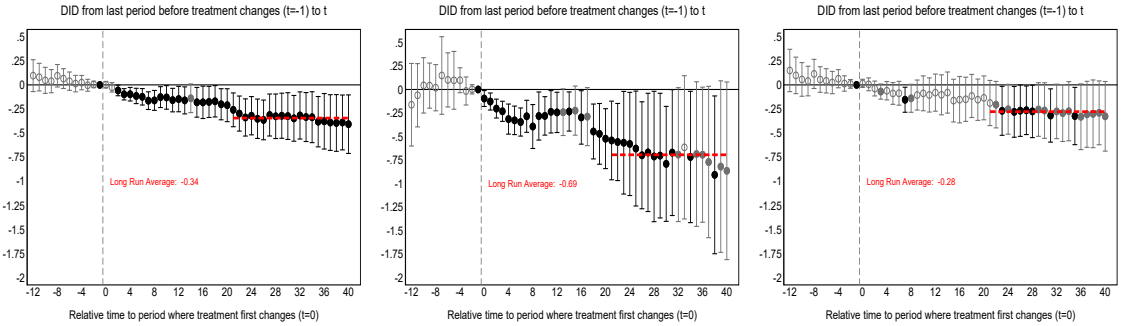

Notes: In these plots, the y-axis shows the values of Equation 1 for the outcome Log Plant Production for 0 to 40 quarters after the plant was flooded for the first time. The pre-trend estimates are computed using the long-difference placebo estimators in de Chaisemartin and D'Haultfoeuille (2022a). The sample comprises production plants that produce 50 units or more during all the quarters between 2000-2019 and did not experience any flooding events on the 28 quarters before the first period in the sample. Standard errors are clustered at the GAUL1 administrative level and computed with 100 bootstrap replications. The circles correspond to the point estimate, the bars correspond to 95% confidence intervals and the colors of the circle mean ● significant at 5%, ● at 10%, ○ not significant at 10%.

Having established that extreme floods have a negative and persistent impact on plant production, I document that firms use their multiplant configuration to offset the drop in an impacted plant's production by shifting production to other unaffected plants. To demonstrate this, first, I use information on the location of production of specific car models, defined by their brand (i.e., Ford), nameplate (i.e., Focus), and body type (i.e., Sedan), to establish which plants are similar within a manufacturer. Then, I define a new treatment variable for each plant that identifies whether one of its sibling plants experienced a flood in a particular period to capture if a plant is indirectly affected by producing at least one of the car models manufactured in a directly affected plant. Finally, I estimate Equation 1 on the subsample of plants with at least one sibling that are active in all the sample periods and do not experience a direct treatment during the sample period or before. Figure 3 reveals that in the long run there is a reallocation of production to other plants that do not experience floods; production increases by around 0.46 log points relative to plants that did not experience any disasters directly or indirectly through the firm's plant network. Although this reallocation is significant, an analysis of total production at the firm level, shown in Figure 3c, reveals that exposure to floods reduces the firm's car production in the medium term. Production drops by about 25% one year after the shock, but eventually recovers.

Finally, I explore how large floods affect the extensive margin of production. I estimate

Figure 3: The Impact of Severe Floods on Unaffected Plants

(a) Direct Effect (b) Indirect Effect (c) Firms' Total Production

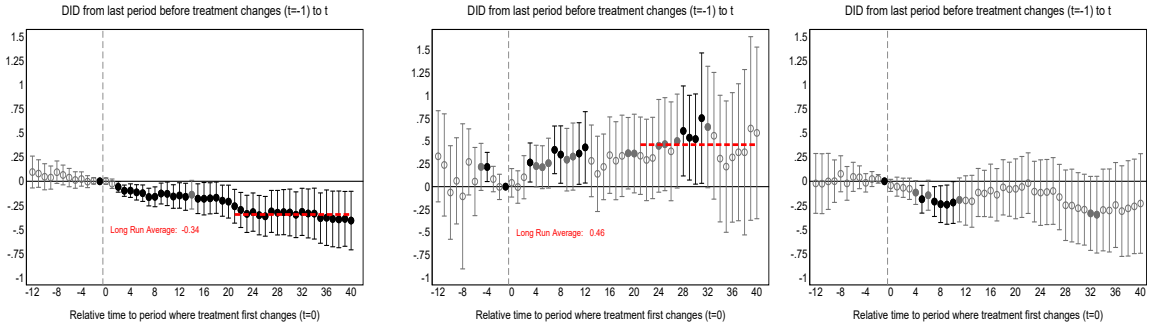

Notes: In this plot, the y-axis shows the values of Equation 1 for the outcome Log Plant Production for 0 to 40 quarters after a related plant was flooded for the first time. The pre-trend estimates are computed using long-difference placebo estimators. Panel (a), is the same plot as Figure 2a. In Panel (b), the sample comprises plants that produce 50 units or more during all the quarters between 2000-2019 and did not experience any flooding events during the sample period or on the 28 quarters before the first period in the sample. In Panel (c), I aggregate plants within the same manufacturer. I only include manufacturers that are actively producing in all the periods in the sample, and produce more than 250 cars in each quarter, and I add pre-sample treatment status as a non-parametric control. Standard errors are clustered at the GAUL1 administrative level in Figures 3(a) and 3(b), and at the firm-level in Figure 3(c) and computed with 100 bootstrap replications. The circles correspond to the point estimate, the bars correspond to 95% confidence intervals and the colors of the circle mean ● significant at 5%, ● at 10%, ○ not significant at 10%.

Equation 1 using as outcome a binary variable equal to 1 if a plant is active in a given period, conditioning on plants that were active in the first period of the sample. Figure B.1a shows that the probability that a plant is active is unaffected by experiencing a flood. In Figure B.1b, I change the unit of observation to GAUL2 regions to document that the number of plants in a location decreases by 0.09 log points after a flood, which is suggestive of firms avoiding these regions when establishing new production plants.

2.4 Robustness

One concern with the estimates above is that the treatment effects captured in Figure 2 could be the result of spillovers between the treatment and control groups, in a potential violation to the Stable Unit Treatment Value Assumption (SUTVA). In my estimation setting, the potential treatment spillovers are observed. To do this, I directly control for floods experienced by other plants within the same firm that produce car models with the same platform, using the estimator proposed in de Chaisemartin and D'Haultfoeuille (2022b).[11] In Figure B.2 in the Appendix, I present the results. The values for these

[11] Production lines within plants are not perfectly substitutable between car models. In most cases, these production lines specialize in producing cars within the same platform as mixed assembly lines cause efficiency losses because of different cycle times and equipment adjustments (see Markus 2021). A platform

estimates are qualitatively and quantitatively similar as the ones depicted in Figure 2.

One could also be worried that the distance threshold of 100km is not correctly capturing the effect of floods on the number of cars produced in a plant. In Figure B.3 of the Appendix, I compute the estimator in Equation 1, but define the flood thresholds at 25km, 50km, 75km, 150km, and 200km. In the cases that I decrease the threshold, the long run averages and the dynamics in these plots are similar to the baseline figure. However, the confidence intervals are somewhat larger, reflecting the fact that as I reduce the thresholds the number of treatments declines rapidly. These findings provide evidence that floods affect car production through local direct and indirect disruptions, not only to the plant itself but to the whole local production environment.

3 Quantitative Model

In this section, I present a model of optimal plant location and capacity investments under uncertainty. Firms choose where to set up their assembly plants, among a set of locations, and invest in capacity in each of those locations. Firms are, potentially, multinational and multiplant, and have the possibility to use their plants as export platforms, as in Helpman et al. (2004) and Tintelnot (2017). Firms choose their horizontal spatial production organization to maximize expected profits before extreme weather disruptions occur. Thus, at the time of their capacity decision, firms do not know the actual productivity of each potential plant location, just the location-specific probability distributions of these productivities. After that, weather events are realized, and firms choose production flows from each of their plants to final markets, conditional on a capacity constraint for each potential location.

3.1 Setup

I model the problem of firm n headquartered in country h_n, with quality equal to γ_n and fundamental productivity equal to ϕ_n. The firm is the owner of a blueprint to produce a single differentiated variety, and chooses in which locations to erect its plants in order to serve multiple markets. I index plant locations by $i = 1, \ldots, I$ and markets by $j = 1, \ldots, J$.

The model is static and the firm makes decisions in two stages. At the beginning of the first stage, firm n knows the value of the triplet of its fundamentals, $\{h_n, \gamma_n, \phi_n\}$, the costs of building capacity in each location, $\{\alpha_{in}\}_{i=1}^{I}$, market-specific demand shifters, $\{\beta_{jn}\}_{j=1}^{J}$, and a vector of firm-location potential plant productivities, $\{z_{in}\}_{i=1}^{I}$. With this information, the firm makes sunk, irreversible investments in capacity in different locations. After these

is a shared set of common design, engineering, and components for distinct car models.

investments are incurred, a vector $\{\kappa_{in}\}_{i=1}^{I}$ of weather shocks that determine the actual productivities of all of its plants is realized. Finally, the firm chooses its production plan to maximize profits conditional on the available capacity and the productivity of each plant.

Geography features in the model in different ways. First, there are bilateral iceberg trade costs that firms have to pay to ship cars across locations. Second, production locations are heterogeneous in their average productivity, average capacity costs, and in the probability of experiencing floods. Finally, the cost of capacity and the productivity of a plant depend on how far the location of a plant is from the firms' headquarters.

3.2 Demand Function and Market Structure

In each market j, consumers have quasilinear preferences over a homogeneous numeraire, Q_0, and a CES aggregator, Q_C, of varieties indexed by ω with elasticity equal to $\sigma > 1$,[12]

$$U_j(Q_O, Q_C) = Q_O + R_j \log \left(\int_{\omega \in \Omega_j} (\psi_j(\omega) q_j(\omega))^{\frac{\sigma-1}{\sigma}} d\omega \right)^{\frac{\sigma}{\sigma-1}}, \tag{2}$$

where R_j measures total expenditure on cars in market j, Ω_j is the set of available varieties and $\psi_j(\omega)$ is a demand shifter specific to variety ω and market j. This demand shifter combines two components; the brand-specific quality γ_n and a home market effect. I further assume that goods of the same variety produced in different origins are perfect substitutes. With these preferences, the demand for variety ω in market j is

$$q_j(\omega) = p_j(\omega)^{-\sigma} \underbrace{\psi_j(\omega) R_j P_j^{\sigma-1}}_{\equiv \beta_j(\omega)^{\sigma}}, \tag{3}$$

where $p_j(\omega)$ is the price of variety ω in country j, and P_j is the ideal price index given by

$$P_j = \left(\int_{\omega \in \Omega_j} \left(\frac{p_j(\omega)}{\psi_j(\omega)} \right)^{1-\sigma} d\omega \right)^{\frac{1}{1-\sigma}}. \tag{4}$$

I summarize total expenditure, the ideal price index, and the demand shifter in a single variable $\beta_j(\omega)$ that measures the size of market j for variety ω. Each good ω is produced by a single firm n under monopolistic competition.

The other consumption good Q_O is homogeneous, freely tradeable, and its consumption is large enough so that it is produced in every single country pinning down wages, w_j. These

[12] This utility for the representative agent can be microfounded by a population of consumers in a country behaving according to a logit discrete choice model à la Anderson et al. (1988).

assumptions imply that the only aggregate variables to solve in the industry equilibrium are the price indices, P_j.

3.3 Production Technology

A firm can produce its variety in I different locations. Each plant can be used to serve the market where it is located and as an export platform. A firm that establishes a plant in a given location makes a sunk irreversible investment in capacity, determining the maximum number of units of goods the firm can produce in all states of the world.

The production function for each plant is linear in its labor input, but the total quantity produced is subject to a capacity constraint. That is,

$$Q_{in} = \underbrace{\kappa_{in}\phi_n z_{in}}_{\equiv \varepsilon_{in}} L_{in} \quad \text{s.t} \quad Q_{in} \leqslant C_{in}. \tag{5}$$

where Q_{in} denotes the total number of cars produced by firm n in location i and ε_{in} is the *ex-post* productivity of firm n in that location. Productivity is the product of three variables: firm n's fundamental productivity ϕ_n, a local productivity z_{in}, both known by the firm at the time of making the capacity investment decision, and a weather disaster, κ_{in}, that is unknown to the firm when choosing its capacity. κ_{in} follows the distribution,

$$\kappa_{in} = \begin{cases} \kappa_1 & \text{with probability } \; r_i \\ \kappa_2 & \text{with probability } \; s_i \\ 1 & \text{with probability } \; 1 - r_i - s_i, \end{cases}$$

with $\kappa_1 < \kappa_2 < 1$ and $r_i < s_i$. This modeling of the weather shocks aims to be parallel to the 10- and 100-year flooding events explored in Section 2. Probabilities are potentially heterogeneous and could be correlated across locations i.[13]

The firm's total production in a given location is the sum of the shipments of that facility to all the potential final markets. Trade of automobiles across space is costly. In order to ship one car from country i to country j, firms need to produce $\tau_{ij} \geqslant 1$ units of the good.

[13] I model extreme weather events using a three-point discrete distribution because it provides a clear mapping between the historical data on floods in Section 2, the model, and the extreme event projections provided by climate models. However, any distributional assumption for the shocks can be chosen for the model as in the solution algorithm I use simulations to approximate expected profits.

Therefore, total production in a plant can be written as,

$$Q_{in} = \sum_{j=1}^{J} \tau_{ij} q_{ijn}, \tag{6}$$

where q_{ijn} is the number of cars that arrive to market j, produced in location i by firm n.

Building capacity in a location is costly. Firm n needs to make an irreversible investment to be able to produce at most C_{in} cars in location i equal to $f_{in}(C_{in})$. The capacity cost function is heterogeneous across locations and firms.

I assume $f_{in}(C_{in})$ satisfies three conditions. First, it is strictly positive for all $C_{in} > 0$. Second, it is strictly increasing in capacity, $f'_{in}(C_{in}) > 0$ for all i, n and $C_{in} \geqslant 0$. This assumption is quantitatively relevant as $f'_{in}(0) > 0$ is required to generate zeros in capacity. Third, I assume that the investment function is weakly convex. In the description of the firm's problem and in the quantitative application, I assume that $f_{in}(C_{in}) = \alpha_{in} C_{in}$.

3.4 The Firm's Problem

The goal of firm n is to choose a production capacity in every location to maximize its expected profits net of the investments incurred in capacity costs.[14] Proceeding by backward induction, I start by describing the *ex-post* problem for firm n conditional on a vector of capacities, $\boldsymbol{C_n} = \{C_{in}\}_{i=1}^{I}$, and location productivities, $\boldsymbol{\varepsilon_n} = \{\varepsilon_{in}\}_{i=1}^{I}$, that is

$$\begin{aligned} \Pi_n(\boldsymbol{C_n}, \boldsymbol{\varepsilon_n}) \equiv \max_{q_{ijn} \geqslant 0} \; & \sum_{j=1}^{J} \beta_{jn} \left(\sum_{i=1}^{I} q_{ijn} \right)^{\frac{\sigma-1}{\sigma}} - \sum_{j=1}^{J} \sum_{i=1}^{I} \frac{\tau_{ij} w_i}{\varepsilon_{in}} q_{ijn} \\ \text{s.t} \; & \sum_{j=1}^{J} \tau_{ij} q_{ijn} \leqslant C_{in} \;\; \forall i \;\; [\nu_{in}] . \end{aligned} \tag{7}$$

This maximization combines an optimal flow problem, in which a monopolistically-competitive firm facing an isoelastic demand has to select both the quantity supplied and the production sources to serve each final market, with a capacity constraint in each potential source facility. The first term in the profit function corresponds to the sum of revenues in every market. The second term captures total production costs. For each potential production location there is a capacity constraint that restricts the amount of goods, inclusive of trade costs, produced in a plant. The variable ν_{in} denotes the Lagrange multiplier associated with the capacity constraint in location i for firm n.

It is worth delving into the role that the variable ν_{in} plays. Economically, ν_{in} quantifies

[14] Appendix G.1 provides a simple model with two locations and one market to study its analytical properties.

the increase in profits from increasing C_{in} marginally, i.e., the shadow value of additional capacity in location i. However, this multiplier also measures the opportunity cost of producing goods in a plant with a binding capacity constraint since serving a market from a particular plant potentially takes away useful capacity profitable for serving other markets.

The profit-maximizing price and quantity in market j are given by

$$p_{jn} = \frac{\sigma}{\sigma - 1} \left(\min_i \left\{ \tau_{ij} \left(\frac{w_i}{\varepsilon_{in}} + \nu_{in} \right) \right\} \right), \tag{8}$$

$$Q_{jn} = \beta_{jn}^{\sigma} \left(\frac{\sigma - 1}{\sigma} \right)^{\sigma} \left(\min_i \left\{ \tau_{ij} \left(\frac{w_i}{\varepsilon_{in}} + \nu_{in} \right) \right\} \right)^{-\sigma}. \tag{9}$$

Firms optimally serve each market from the plant with the cheapest marginal cost. The cost of supplying a market depends on both the transportation cost and on the marginal production cost in the source plant. Note that the marginal cost is augmented by ν_{in} to reflect the true cost of producing an additional unit in plant i.[15]

The *ex-ante* capacity choice problem of firm n consists on choosing the location and the capacity of its production plants to maximize expected profits net of investment costs. It is given by

$$\max_{C_{in} \geqslant 0} \ \mathbb{E}_{\boldsymbol{\varepsilon_n}} \left[\Pi_n(\boldsymbol{C_n}, \boldsymbol{\varepsilon_n}) \right] - \sum_{i=1}^{I} \alpha_{in} C_{in}. \tag{10}$$

The first term corresponds to the expected operating profits when the vector of capacities is equal to $\boldsymbol{C_n}$. The second term denotes the total investment cost of the installed capacity.

From the envelope theorem, the first order condition for the variable C_{in} is given by

$$\mathbb{E}_{\boldsymbol{\varepsilon_n}} \left[\nu_{in}(\boldsymbol{C_n}, \boldsymbol{\varepsilon_n}) \right] \leqslant \alpha_{in}, \tag{11}$$

with equality if firm n builds a plant in location i. A firm will invest in capacity in location i until the expected marginal increase in profits due to an increase in capacity equals the marginal investment cost. In addition, this optimality condition elucidates under which circumstances the firm does not set up a plant in some location. This occurs if the expected marginal benefit from investing an infinitesimal amount in location i, with optimal capacities elsewhere, is strictly smaller than the marginal cost of investment at 0, $f'_{in}(0) > 0$. Lastly, it is easy to see that if a firm invests on capacity in i, it must be the case that there is a

[15] In this model, it is possible that a market is served by more than one plant. In this case, the marginal cost of serving that market must be equalized across those plants. The Lagrange multipliers of these plants adjust in such a way that marginal costs are the same.

measure of states of the world, in which the capacity constraint for plant i is binding, as reflected by the fact that the expectation of ν_{in} needs to be positive, if $C_{in} > 0$.

These first-order conditions help understand the incentives to invest in resilience. When a flood affects plant i, ν_{in} decreases; as the plant becomes less productive, while the multipliers in the unaffected plants weakly increase as their capacity becomes scarcer. When the probability of disruptions in i rises, events with a smaller value of the multiplier become more frequent, decreasing the expected marginal returns of investment in i and weakly increasing them elsewhere. Capacities adjust to restore Condition 11 for all i.

3.5 Solution Strategy

This model requires solving interdependent capacity choices among numerous locations, further complicated by a high-dimensional expectation, making it computationally challenging. However, as I first show, this problem is convex ensuring its numerical tractability.

Proposition 1 *The* ex-ante *capacity choice optimization problem of the firm is a concave objective function defined on a set of linear constraints.*

Proof *See Appendix C.1.*

Since the problem is convex, any locally optimal point is also globally optimal. Karush-Kuhn-Tucker (KKT) conditions assure global optimality and enable the use of large-scale optimizers that converge to the unique global optimum (Boyd and Vandenberghe 2004).

I use S random samples drawn from the probability distribution of $\boldsymbol{\varepsilon_n}$ to approximate the high-dimensional expectation. By averaging these samples, I compute expected profits for a specific capacity vector $\boldsymbol{C_n}$. Precisely,

$$\mathbb{E}_{\boldsymbol{\varepsilon_n}}\left[\Pi_n(\boldsymbol{C_n}, \boldsymbol{\varepsilon_n})\right] \approx \frac{1}{S}\sum_{s=1}^{S} \Pi_n(\boldsymbol{C}_n, \boldsymbol{\varepsilon}_n^{\boldsymbol{s}}).$$

I exploit the convexity and the inherent structure of the firm's problem to transform it into an equivalent, efficiently solvable maximization problem. By Propositon 1, this problem admits strong duality.[16] Next, I introduce the dual problem for firm n.[17,18]

[16] Strong duality follows from the convexity of the optimization problem and the linearity of the constraints. Due to these two properties, Slater's condition holds which is sufficient for strong duality.

[17] The study of dual nonlinear programming problems in economics can be traced back to Balinski and Baumol (1968) which shows that if the primal problem is characterized by diminishing returns, which in this problem comes from the concavity of the profit function with respect to quantities, the standard dual properties apply.

[18] In Appendix C.2, I derive the dual for particular nonlinear capacity cost functions, and provide a solution algorithm for arbitrary convex capacity cost functions.

Proposition 2 *The dual ex-ante optimization problem of firm n is*

$$\min_{\nu_{ins} \geqslant 0} \frac{\left(\frac{\sigma-1}{\sigma}\right)^{\sigma-1}}{\sigma} \sum_{s=1}^{S} \sum_{j=1}^{J} \frac{\beta_{jn}^{\sigma}}{S} \left(\min_{i} \left\{ \tau_{ij} \left(\frac{w_i}{\varepsilon_{ins}} + \nu_{ins} \right) \right\} \right)^{1-\sigma} \tag{12}$$

$$s.t \ \ \frac{1}{S} \sum_{s=1}^{S} \nu_{ins} \leqslant \alpha_{in} \ \ [C_{in}] \ \ \forall i$$

Proof *See Appendix C.1.*

In the dual problem, the vector $\boldsymbol{\nu_n}$ is chosen to minimize the expected economic rents appropriated by the owner of the firm, consistent with Balinski and Baumol (1968). The constraints of the problem coincide with Equation 11, and reflect that in the optimum the marginal benefit of additional capacity must be weakly lower than its marginal cost. Crucially, the multipliers of each constraint correspond to the optimal values of capacity.

The problem in Proposition 2 is still numerically challenging as it is nonlinear and not continuously differentiable. However, as I show next, with a change of variables, the problem can be reformulated into an equivalent convex problem with a linear objective function.

Proposition 3 *The dual optimization problem described in Proposition 2 can be written as the minimization of a linear objective function on a convex set as*

$$\min_{\nu_{ins}, \mu_{jns}, t_{jns} \geqslant 0} \frac{\left(\frac{\sigma-1}{\sigma}\right)^{\sigma-1}}{\sigma} \sum_{s=1}^{S} \sum_{j=1}^{J} \frac{\beta_{jn}^{\sigma}}{S} t_{jns} \tag{13}$$

$$s.t \ \ \sum_{s=1}^{S} \frac{\nu_{ins}}{S} \leqslant f'_{in}(C_{in}) \ \ \forall i; \ \ \mu_{jns} \leqslant \tau_{ij} \left(\frac{w_i}{\varepsilon_{ins}} + \nu_{ins} \right) \ \ \forall i, j, s; \ \ (t_{jns}, \mu_{jns}, 1) \in P_3^{\frac{1}{\sigma}, 1-\frac{1}{\sigma}} \ \ \forall j, s$$

where $P_3^{\frac{1}{\sigma}, 1-\frac{1}{\sigma}}$ denotes a three-dimensional power cone.[19]

Proof *See Appendix C.1.*

This reformulation allows me to solve the firm's problem introduced in Equation 10 very quickly. The problem in Equation 13 belongs to the class of conic optimization programs, a nonlinear extension of conventional Linear Programming optimization, that can be solved in polynomial-time and has a well-developed duality theory (see, e.g., Letchford and Parkes 2018 and MOSEK ApS 2023). State-of-the-art optimizers have streamlined routines that solve these problems with hundreds of variables and constraints in less than a second.[20]

[19] $P_3^{\alpha,1-\alpha}$ is a convex set defined as $P_3^{\alpha,1-\alpha} = \left\{ x \in \mathbb{R}^3 : x_1^{\alpha} x_2^{1-\alpha} \geqslant |x_3|, x_1, x_2 \geqslant 0 \right\}$.

[20] I solve this problem using the optimizer `Mosek` implemented on `Julia` through the optimization modeling language `JuMP` (see, respectively, MOSEK ApS 2022, Bezanson et al. 2017 and Lubin et al. 2023).

4 Empirical Results

In this section, I describe, the data used estimating the model, the estimation strategy, and the parameter estimates and their quantitative implications.

4.1 Structural Estimation Data

I use three types of data. First, I use the car registration dataset described in Section 2. Since the model is static and the burden of solving it is considerable, I aggregate the data at an annual level and I use 2019. For each plant, I construct flows to each destination market.

I complement the car registration data with list price data (MSRPs) in 2018 and 2019 for China, Brazil, Germany, Mexico, Japan, India and the United States, at the car model level. To these price data, I merge the location where the car models were produced to estimate trade costs. I use this dataset to estimate the demand block of the structural model, by adding bilateral applied tariffs for each pair of countries sourced from ITC (2022), and standard bilateral gravity measures from CEPII (Mayer and Zignago 2011).

To estimate the model, I need to define the geographical units at which firms make their choices. Firms' choices need to be made at subnational units of aggregation, as different regions within countries are affected in dissimilar ways by climate change. I define these subnational units using GAUL1 units. The locations included in the estimation of the model appear in blue in Figure A.3, and correspond to locations with car production in 2019.[21]

For each location, I collect a number of variables that proxy for the local fundamental productivity and the local cost of investment in capacity. I source population counts in 2020 for each 1km grid from WorldPop (2021). From Kummu et al. (2018), I retrieve location-specific estimates of GDP per capita for 2015. I construct measures of road density using data from Meijer et al. (2018) by averaging highway and primary road density for each cell. As a proxy for the price of land in each administrative unit, I construct measures of land availability. by computing the share of undeveloped land, with a slope smaller than 15%, following Saiz (2010). I obtain information about global land use from Zanaga et al. (2021). Finally, I use the geographical coordinates of the centroid of each location to compute bilateral distances to the population-weighted centroid of each country.[22]

[21] In the counterfactuals in Section 5, I expand the locations in the firms' choice set to all the GAUL1 units in the countries for which there are sales. These locations are colored in green in Figure A.3 in the Appendix.

[22] I provide more details about the data construction and show maps with the resulting data in Appendix A.2.2.

4.2 Econometric Specification and Estimation Strategy

I estimate the model in two steps. First, I estimate trade costs and demand. Second, I estimate the parameters that govern the productivities and investments costs in each location and the values of the productivity penalties from experiencing a flood.

4.2.1 Trade Costs

To estimate trade costs, I draw on matched data on prices and the location of production of models and use Equation 8, the optimal price equation derived from the model.

I interpret differences in prices of specific car models that are produced in the same plant, and sold in different markets as being driven by trade costs τ_{ij}.[23] I assume $\tau_{ij} = (1 + \text{tariff}_{ij})^{\phi_{tar}} d_{ij}^{\phi_{dist}}$, where tariff_{ij} denotes car tariffs and d_{ij} denotes distance between locations i and j. The parameters ϕ_{tar} and ϕ_{dist} are estimated from the regression:

$$\log(p_{ijm}) = \phi_{tar} \log(1 + \text{tariff}_{ij}) + \phi_{dist} \log d_{ij} + \alpha_{im} + \alpha_j + u_{ijm}. \tag{14}$$

The model-plant fixed effect, α_{im}, controls for the unobserved marginal cost for model m in location i, subsuming the fundamental productivity of the firm, wages, firm-origin specific shocks, and the multiplier associated to the capacity constraint. The destination-specific fixed effect α_j controls for market-specific measurement error. The estimate of ϕ_{tar} is 0.834 (robust S.E equal to 0.075) and for $\phi_{dist} = 0.033$ (robust S.E equal to 0.004).

4.2.2 Demand Elasticity, Home Market Effects, and Brand-Specific Quality

Consider the demand function described in Equation 3 in logs,

$$\log Q_{jn} = -\sigma \log p_{jn} + \log R_j + (\sigma - 1) \log P_j + \log \psi_{jn} + \sigma u_{ijn}. \tag{15}$$

I assume that the demand shifter ψ_{jn} is made up of a firm-specific quality term γ_n and a home bias component. Thus, $\log \psi_{jn} = \gamma_n + \vartheta BrandHome_{jn}$.

Given that the data comes at the model level but the relevant elasticity of substitution from the perspective of the model is across varieties of different firms, I assume a nested CES demand to collapse models of the same firm into quantity- and price-composites at the firm level. First, I estimate the following share regression at the model-market level,

$$\log s_{jmn} = (1 - \sigma_m) p_{jmn} + P_{jn} + v_{jmn}^m. \tag{16}$$

[23] See e.g. Anderson and van Wincoop (2004), Atkin and Donaldson (2015) and Donaldson (2018).

where s_{jmn} is the sales share of model m within brand n in market j, and P_{jn} is the ideal price-composite for firm n in market j.[24] Then, I use another share regression at the firm-market level to estimate σ across firms including the demand shifter ψ_{jn},

$$\log s_{jn} = (1-\sigma)P_{jn} + \gamma_j + \gamma_n + \vartheta BrandHome_{jn} + v^n_{jn}. \tag{17}$$

In Table D.1, I present the results from estimating Equations 16 and 17. In the preferred specification, I estimate a demand elasticity across models of the same firm of 4.3 and across firms of 2.6 and a home market effect of around 1.0. The demand elasticity across models is quite similar to the one obtained in Head and Mayer (2019), who estimate an elasticity of 3.9, without price data. The home market effect is in line with Coşar et al. (2016) and is substantial.[25]

4.2.3 Market-Specific Shifters

To estimate the component of the firm-market shifters β_{jn} that is specific to market j, which I denote by δ_j and captures aggregate expenditure and the price index in that market, I also use the structural demand equation. However, I need to compute a different regression than in Equation 17, because I cannot retrieve shifters for all markets due to lack of data on prices. Instead, I substitute the optimal pricing equation in the demand and estimate:

$$\log Q_{ijm} = \delta_1 \log(1+\text{tariff}_{ij}) + \delta_2 \log d_{ij} + \delta_{im} + \delta_j + \vartheta^{ms} BrandHome_{b(m)j} + \gamma^{ms}_{n(m)} + \varepsilon_{ijm}. \tag{18}$$

In Figure D.2, I show the estimates of δ_j. These shifters are the largest in markets with a large population and high income, e.g. United States or China.

4.2.4 Distributions of Productivities, Capacity Costs and Flood Damages

Given the estimates for trade costs and the demand equations, I use a Simulated Method of Moments (SMM) estimator to obtain estimates for the determinants of z_{in} and α_{in}. I cannot use the model's structural equations to recover them using a saturated regression

[24] To estimate the elasticity in Equation 16, I use tariffs as an instrument for prices. An instrument is needed because I assume that prices are observed with measurement error, and because, in this model, marginal costs are not constant, and therefore, prices are affected by the structural determinants of quantities.

[25] In Figure D.1, I present correlations of $\hat{\gamma}_n$ with prices, as well as the distribution of shifters by the home market of the firm. These brand shifters should be interpreted as measures of quality that explain why the demand for some brands is larger than for others after controlling for prices and home market effects.

or a model inversion. Therefore, I treat them as structural errors that come from known parametric distributions, and I estimate the parameters of these distributions.

I assume that both errors follow Log-Normal distributions. Precisely, I assume that z_{in} and α_{in} are drawn from the distributions $F^z_{in}(z_{in}) = \log\mathcal{N}(X'_{in}\delta^z + G'_i\delta^w, \xi^z)$ and $F^\alpha_{in}(\alpha_{in}) = \log\mathcal{N}(X'_{in}\delta^\alpha, \xi^\alpha)$, respectively. Conditional on the vectors X_{in} and G_i, I assume that these draws are independent across firms and locations. I linearly project the mean on a vector of observable characteristics that attempt to proxy for fundamental determinants of productivity and investment costs.[26] In contrast, I assume that for both distributions the dispersion parameters ξ^z and ξ^α are common across firms and locations.

I use a parsimonious set of observable characteristics contained in vector X_{in} to model these distributions. The vector X_{in} includes a constant, local measures of log gross domestic product per capita, log population, and log road density, a home market dummy, the distance between location i and a firms' country of origin, and a measure of local land availability. I subsume the vector of wages in each location by adding the term $G'_i\delta^w$, where G_i are dummy variables that denote whether a particular location belongs to a country in one of six GDP bins, allowing productivity levels to flexibly vary across groups. Then, I use the structural model to estimate the parameters $\delta^z, \delta^w, \delta^\alpha, \xi^z$ and ξ^α.

I use the Simulated Method of Moments (SMM) to estimate the vector of parameters $\Theta = \{\delta^z, \delta^\alpha, \delta^w, \xi^z, \xi^\alpha, \kappa_1, \kappa_2\}$ following Gourieroux et al. (1993). The estimation procedure uses the model described in Section 3 as a data generating process that simulates a set of production and location choices for a set of artificial firms for a candidate parameter vector $\tilde{\Theta}$, and S vectors of simulations draws for the structural errors. These endogenous choices are translated into moments and averaged out across simulations. Then, the estimator finds the value of $\tilde{\Theta}$ for which the distance between the vector of moments in the data, and their simulated counterpart when the parameters are equal to $\tilde{\Theta}$, is minimized.

Forty-eight empirical moments are chosen as targets for estimation.[27] Since the model is over-identified, variation in all the moments jointly determines all the parameters of the model. However, different sources of variation in these moments are more informative for some of the parameters and are associated with the identification of different parameters.

I use three blocks of moments. The first block is geared towards matching the spatial distribution of plants and production. I define moments that interact X_{in} and G_i with $\log Y_{in}$, log production in location i by firm n, and with D_{in}, a binary variable equal to 1 if

[26] Another option would be to be fully flexible and estimate a mean by location, akin to a fixed effect. However this would require the estimation of a high-dimensional vector that is computationally infeasible and that would likely produce noisy estimates given the granular level of the data.

[27] In Table E.1, I present the explicit equations for the estimation moments.

firm n has a plant in location i.[28]

The second group of moments match features of the distributions of firm-level production and number of plants. I include as moments the average of the logs of the total number of plants and of total production, as well as the squares of those logarithms. Also, I incorporate moments that attempt to match various percentiles of the distributions of total production and total number of plants by firm, and features of their joint distribution. Finally, I include moments to match the average difference between the production of the largest plant and the second largest plant across firms with multiple plants and the average production of the largest plant.

To estimate the flood damage parameters κ_1 and κ_2, I simulate flood realizations within the model and I compare a plant's production with and without floods, holding the fundamentals and the capacity fixed. I simulate floods using the definition of 10-year and 100-year floods, assuming these occur with a 10% and 1% probability, respectively, and match the model-implied responses to the long-run averages from Figure 2.

4.3 Results of the Structural Estimation

In Table D.2, I show the results of the structural estimation. The standard errors are computed using the usual formula for simulated method of moments estimators provided in Gourieroux et al. (1993). In Appendix E.2, I discuss the fit of the model.

Starting from the determinants of the capacity costs, α_{in}, the estimates suggest that in locations with a larger population, with higher road density, with large GDP per capita, and with less available land, the expected cost of a unit of capacity is larger. Due to the expression for the expectation of the Log-Normal distribution, these estimates can be interpreted as elasticities. An increase of 1% in the population, road density, and GDP per capita of a location decrease the expected cost of capacity by 0.02%, 0.01% and 0.05%, respectively. The coefficient on land availability can be interpreted as a semi-elasticity; an increase in 1 percentage point in the share of available land in a location decreases the expected cost in 0.12%. I find important home market effects in the cost of capacity. All else equal, the cost of a unit of capacity in the headquarters country of the firm is 27.7% smaller than in any other country. This home market effect is amplified by the fact that the costs of capacity increase, with an elasticity of 0.05%, as locations are farther away from the headquarters country of the firm.

The expected productivity of a location, z_{in}, increases by 0.03%, 0.03%, 0.07% and

[28] I discuss the separate identification of the productivity and the capacity cost parameters in Appendix G.2.

decreases by 0.052% with a 1% increase in population, road density and GDP per capita, and with a 1 p.p increase in land availability. Productivity is on average 22.7% larger for locations within the firms' home country and I find gravity in productivity; an increase in distance away from the home market reduces productivity with an elasticity of 0.04%.

I find sizable productivity penalties as a consequence of floods. To rationalize the impact of floods on car production estimated in Figure 2 through the model, the productivity after a 100-year flood decreases by approximately 75% and after a 10-year flood by 60%.

It is difficult to gauge the economic implications of the magnitude of these estimates from the numbers alone. In Figures 4 and 5, I explore the implications of these estimates for productivities, investment costs and the location of production.

In Figure 4a, I plot the average productivity for each GAUL1 administrative unit in the sample of U.S firms. I condition on firms from a particular origin as productivities and capacity costs are partly determined by the home country of each firm. The estimates reveal that the most productive locations are in the developed world, in places such as the United States, Canada, and Western Europe, reflecting the prominence of GDP per capita as a determinant of local car production productivity. However, what matters for production is how these productivity measurements interact with the estimated costs of labor and the costs of capacity investment. In Figure 4b, I plot the average marginal cost of production in each location for American firms. Once one takes into account differences in wages across locations, the places with the smallest marginal costs are locations such as India, South America and Mexico. Furthermore, these estimates reveal that home market effects are very relevant in determining productivities.

In Figure 4c and Figure 4d, I plot the average costs of investing in capacity for American and German firms, respectively. From these maps, it is clear that home market effects are important, as the cheapest country for investing for firms from both origins is their origin, whereas investing in Europe, for the U.S firms, or in the United States, for German firms, seems very expensive highlighting that these investment costs are increasing in local income. The map shows that the capacity costs increase in distance to headquarters. For instance, for U.S firms capacity is cheaper in Mexico than in South America. Likewise, for German firms, capacity is cheaper in France than in Canada.

Figure 5 presents the geographical distribution of production and of plants as implied by the model. Ultimately, where firms decide to locate their plants and produce their goods is a function of three determinants. Due to the existence of trade costs, firms want to be close to large markets as measured by the firm-specific market shifter β_{jn}, at the same time that they produce in places that minimize the costs given a level of capacity and the costs

Figure 4: Implications of Parameter Estimates

(a) Average Productivity - U.S Firms

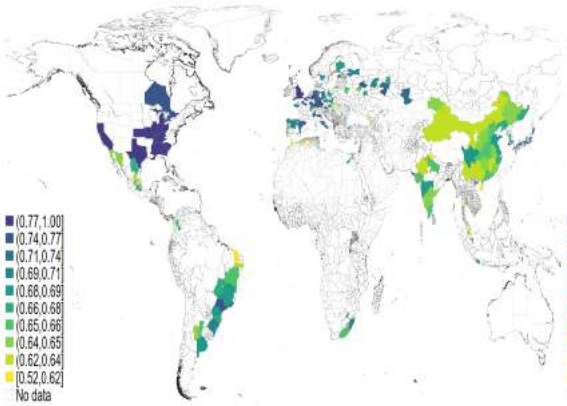

(b) Average Marginal Cost - U.S Firms

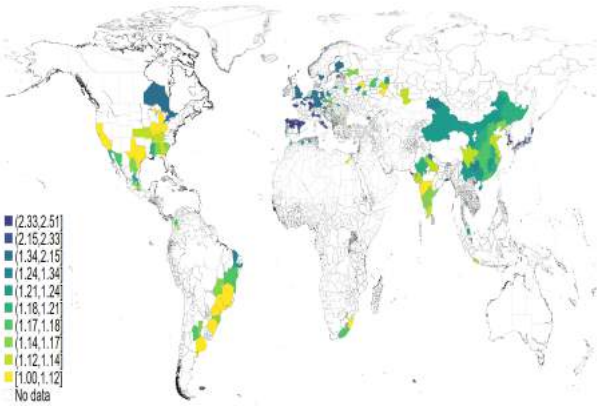

(c) Average Costs of Investing in Capacity - U.S Firms

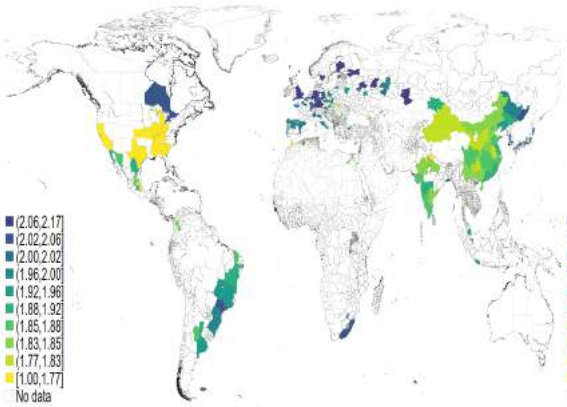

(d) Average Costs of Investing in Capacity - German Firms

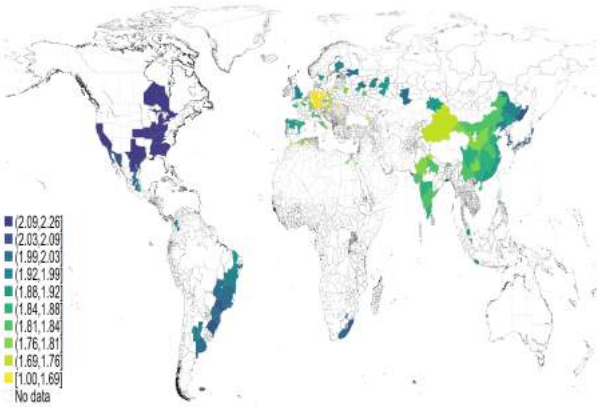

Notes: These maps show the values of average productivities and marginal costs for American firms, and average capacity costs for U.S and Japanese firms respectively. The values are normalized by the location with the largest productivity in Panel (a), and by the location with the smallest value in the others.

Figure 5: Model Implied Location of Production and of Plants

(a) Number of Produced Units (b) Number of Plants

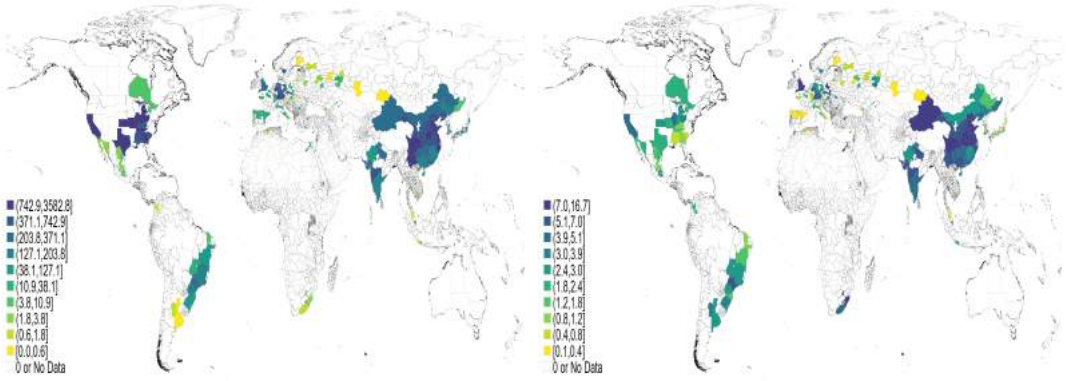

Notes: These maps show the number of cars (in thousands) and the number of plants generated by the model across 100 simulations. The locations taken into account correspond to the GAUL1 units where there is car production in 2019.

of building that capacity, and they want to have multiple firms to serve those markets in such a way that there production is resilient. The model predicts that plants locate mostly in North America, Central Europe, in particular in Germany and the Northeast of France, China and Japan. The places in which the model predicts production strikingly resemble where production takes place in the data. In Figure A.2 in the Appendix, I show the number of plants and cars produced in the data for 2019.

5 The Effect of Changes in the Probability of Floods on Firm Organization

In this section, I evaluate how firm-level plant location, number, and capacity decisions respond to changes in the likelihood of extreme weather events and the implications of these responses for the industry's location of production, average productivity, and consumer prices. The main counterfactual is to modify the probability distribution of extreme weather events and recompute firms' choices by combining the estimated structural model with projected probabilities for extreme precipitation events from climate models.[29]

[29]This exercise makes certain assumptions which are consequential for the results. First, I assume the future production damage from floods, will remain the same as the one based on historical data, disregarding other potential adaptation mechanisms beyond plant reorganization that could mitigate flood impacts. Second, the focus is exclusively on extreme flooding events, abstracting from other climate change effects such as permanent shifts in average temperature and precipitation that could affect locations heterogeneously, and other potential climate-change-induced disasters like droughts and wildfires, which might either contrast or compound with floods.

5.1 Projected Probabilities of Extreme Weather Events under Climate Change

I draw upon climate projections from Coupled Intercomparison Project Phase 6 (CMIP6) models to inform changes in probabilities of a weather disaster in a specific location. These projections are based on alternative emission scenarios, known as Shared Socioeconomic Pathways (SSPs), that attempt to capture possible pathways for societal development.[30]

I define a flood disaster as a five-day rainfall event that exceeds the location-specific historical thresholds for 10-year and 100-year return periods (which historically occur with 10% and 1% probabilities, respectively). I measure the yearly probability of these events occurring during 2035-2064 under a specific Shared Socioeconomic Pathway, using projections from a multi-model ensemble based on CMIP6 protocols. These probabilities come from the World Bank's Climate Change Knowledge Portal, provided on a $1^o \times 1^o$ global grid and aggregated using a simple average at the GAUL1 level.[31]

In SSP5-8.5, the average probability in 2050 of a 10-year event becomes 14.6% and of a 100-year event 1.9% with climate change. However, these probabilities are spatially heterogeneous due to the differences in geography, topography, and position in the globe of distinct locations.[32] For instance, in SSP5-8.5, the probabilities of a 100-year event are expected to increase in Tennessee to 2.2%, in Michigan to 2.3%, and in Tokyo to 1.4%, whereas the probability in Tangier, Morocco decreases to 0.8%. In SSP3-7.0, the probabilities of extreme events in these places are 2.5%, 1.9%, 1.7%, and 0.7%. In Figure 6, the probabilities for 10-year extreme precipitation events are illustrated in Panel (a), while 100-year events are depicted in Panel (b). These maps reveal significant heterogeneity in these probabilities. For instance, regions in North Africa, Turkey, and Spain are anticipated to experience a decrease in the likelihood of extreme precipitation; conversely, in areas in Central Africa and Southeast Asia, a fivefold increase is projected.

5.2 Baseline Predictions

Table 1 documents how different assumptions on the distribution of climate change shocks affect the firms' organization of production. Four patterns emerge. First, as the probability

[30] See IPCC (2021a) for an exhaustive description of the five main Shared Socioeconomic Pathways. In this paper, I focus on (1) SSP1-1.9, the low end of future emission, (2) SSP3-7.0, a medium to high range emissions scenario; and (3) SSP5-8.5, a high-end of emissions and of warming worst-case scenario.

[31] See World Bank Group, Climate Change Knowledge Portal https://climateknowledgeportal.worldbank.org/.

[32] According to the IPCC (2021b), precipitation is projected to increase over high latitudes, the equatorial Pacific and parts of the monsoon regions. Global warming will intensify the global water cycle and the severity of precipitation events.

Figure 6: Extreme Precipitation Probabilities under SSP55-8.5

(a) 10-Year Event (b) 100-Year Event

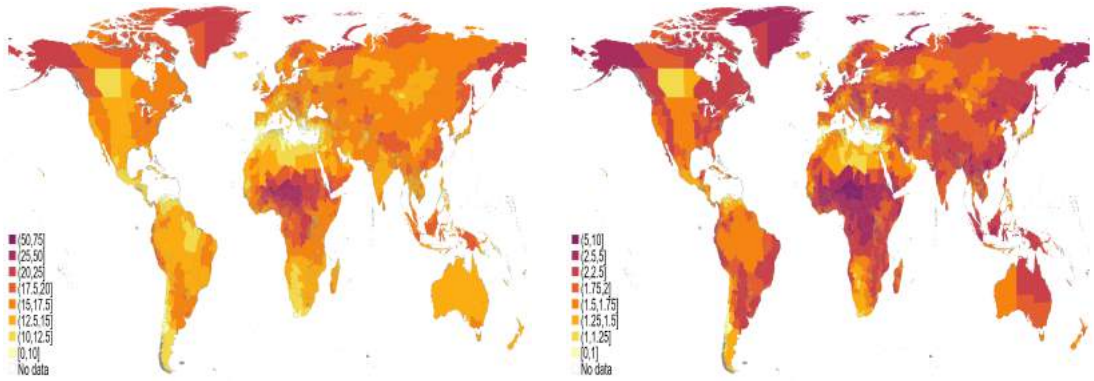

Notes: These maps show the probability of historical 10-year precipitation events in Panel (a) and 100-year precipitation events in Panel (b). These projections come from a multimodel ensemble for SSP5-8.5 from the Climate Change Knowledge Portal of the World Bank. The administrative units in the map correspond to GAUL1 units.

of adverse weather shocks to productivity increases, firms produce in more locations, but the capacity of these plants shrinks. That is, firms, on average, operate with a larger number of smaller plants. Comparing the current scenario, where 100-year and 10-year events happen with probabilities of 1% and 10%, and SSP5-8.5, the average firm increases its number of plants by 4.4%, but average capacity per plant decreases by 7.2%.

Second, firms shrink. For the average firm, production capacity declines by 4.9% and profits by 4.1% between the current scenario and SSP5-8.5. In the counterfactual, the likelihood of an event that reduces productivity increases, and therefore, the expected productivity of each location is smaller. Hence, firms expected productivity declines, reducing their incentives to invest in size. Moreover, firms reallocate production capacity from ex-ante productive locations to places that are less productive, but give them the option to hedge. This implies a further decline in size as firms organize production in a more dispersed way across space, losing the productivity gains from concentrating production in the locations that produce at the expected lowest cost.

Third, firms operate with more spare capacity. In a counterfactual world without shocks, firms operate at full capacity as there are no sources of uncertainty. As climate change becomes more severe, firms start to hold more spare capacity to accommodate potential shocks to their other plants. This means that firms invest in resilience, even if most of the time, this spare capacity is not used. The benefit of expanding production in a plant if production in an affiliated plant is disrupted outweighs the cost of excess capacity if this additional capacity is idle or, even worse, if the plant itself suffers an adverse productivity

event. In SSP5-8.5, firms reserve 7.0% of their total capacity for such hedging purposes.

Table 1: Firms' Plant Structure over Different Climate Change Scenarios

Extreme Precipitation Probability	**0%**	**1%/10%**	**SSP1-1.9**	**SSP3-7.0**	**SSP5-8.5**
Average Number of Plants	7.08	6.49	6.63	6.77	6.78
Average Capacity per Firm	513.61	465.52	451.97	446.34	442.92
Average Capacity per Plant	205.02	152.93	149.17	141.27	141.91
Average Profits	9258.91	8546.81	8259.24	8264.50	8214.25
Percentage Change	8.1%	0.0%	-3.57%	-3.51%	-4.09%
% Negative Profits	0.00%	0.42%	0.66%	0.52%	0.55%
Average Used Capacity	100.0%	95.3%	93.7%	93.4%	93.0%
Average Capacity HHI	1.000	0.882	0.852	0.833	0.825
Average Production HHI	1.000	0.884	0.855	0.835	0.828

Notes: This table shows different statistics about the firms' plant organization over different climate scenarios. For each column, I am assuming firms make their capacity choices assuming different probabilities for extreme weather events, and that those events are generated according to those probabilities. In the first column, extreme events do not happen. In the second column, 10-year events happen with a 10% probability and 100-year events happen with a 1% probability. This is the baseline scenario used to estimate the model. In columns 3 to 5, extreme weather event probabilities correspond to those in SSP1-1.9, SSP3-7.0 and SSP5-8.5, respectively. Statistics about capacity are in thousands of cars. Statistics about profits and investment are in millions of dollars.

Finally, both capacity and production become less spatially concentrated as measured by the HHI. This follows directly from the fact that firms are spreading their plants and their production capacity in space in order to diversify against the extreme weather shocks.

In Table 2, I explore the extent to which the reconfiguration of the firms' production structure is an effective as adaptation mechanism to negative shocks. To do this, I compare profits when firms reorganize their plants in reaction to a change in the probability of these shocks, with profits in a case in which shocks occur according to the new probabilities, but firms' choices are held fixed to the ones before climate change. I find that under different climate scenarios, adaptation substantially reduces the decline in profits caused by climate change. For instance, the profits of the average firm decline by 4.1% between the current risk landscape and SSP5-8.5 when firms optimally adapt. However, when the probabilities of floods change but firms do not adapt, the corresponding decline in profits is of 5.3%. That is, adaptation reduces the loss in profits due to climate change by around 20%. This finding is consistent for the most severe climate change scenarios.

The implications of firms' plant reorganization in SSP5-8.5 for the spatial allocation of automobile production are heterogeneous across countries as shown in Figure 7a. Globally, production declines by 6.6%. In most countries, production declines; however, there is a group of countries, such as Morocco, Egypt, South Africa, Italy, and Mexico, that experience an increase in the number of cars produced. Most of the reallocation of production takes

Table 2: Effects of Adaptation on Profits

Extreme Precipitation Probability	**0%**	**1%/10%**	**SSP1-1.9**	**SSP3-7.0**	**SSP5-8.5**
Average Profits with Adaptation	9258.91	8546.81	8259.24	8264.50	8214.25
Relative to 1%/10%					
Decrease in Profits with Adaptation			-3.6%	-3.5%	-4.1%
Average Profits without Adaptation			8255.08	8175.54	8110.10
Decrease in Profits without Adaptation			-3.6%	-4.5%	-5.3%
Losses from not adapting			-0.1%	-1.1%	-1.3%
Share of Losses Averted			1.4%	22.9%	22.9%

Notes: This table shows different statistics about firms' profits with and without adaptation over different climate scenarios. In the first row, I compute profits when firms adapt by choosing plant locations and capacities according to the probabilities for extreme weather events in the column. I compute profits when I hold fixed the capacity choices that are optimal when weather events happen with 1%/10% probability, but the events are generated with the probability corresponding to the column.

place within countries and trading blocs.

In Figure D.3, I present changes in production shares within a country for the largest 10 producers. Take the United States as an example. In Figure 7a, we see that production in the United States exhibits a considerable decline of 7%. Nonetheless, as Figures 7b and D.3 show, this decline in production is mostly driven by changes in the location of production within the US; production is moving from very productive regions in the Southeast, the Midwest and the Great Lakes (e.g. Michigan and Tennessee), for which extreme precipation probabilities are increasing considerably, to locations in the Great Plains (e.g. Nebraska and Kansas) that are less productive. These stark reallocation patterns appear within other countries as well. For instance, as shown in Figures 7b and D.3 in Germany, Spain and France, there is a reallocation of production towards the Southern part of these countries, in China, production reallocates from the more tropical south to the North, and in India, production reallocates towards the Center.

The impacts of climate change on production are mimicked by changes in total capacity, as seen in Figure 8a. Total global capacity shrinks by 4.9%. Firms shrink capacity in countries that become more affected by climate change and expand capacity in countries that are less affected. However, this adaptation mechanism interacts with market access in subtle ways as firms do not substitute locations without considering how the new potential sites impact their market access. Most of these substitutions take place between locations that are close to each other.

Figure 9a exhibits the impact of climate change on car price indices in each country. Following the model in Section 3, increases in price indices are sufficient statistics for the

Figure 7: Log Change in Production for SSP5-8.5

(a) Country Production

(b) GAUL1 Production

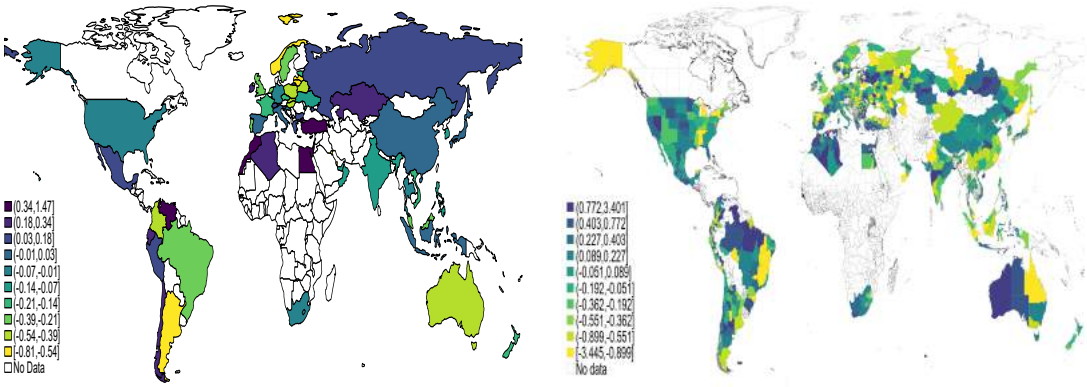

Notes: These maps show log changes in the number of cars produced between the current risk landscape, where 10-year floods occur with 10% probability and 100-year floods have a 1% probability, and the projected probabilities for SSP5-8.5, at the country-level in Panel (a) and at the GAUL1-level in Panel (b). Quantities are averaged across 100 simulations of the structural errors. The estimates used to simulate the model are in Table D.2. The probability projections used come from a multimodel ensemble for SSP5-8.5 from the Climate Change Knowledge Portal of the World Bank. The administrative units in the map correspond to GAUL1 units.

Figure 8: Log Change in Capacity for SSP5-8.5

(a) Country Capacity

(b) GAUL1 Capacity

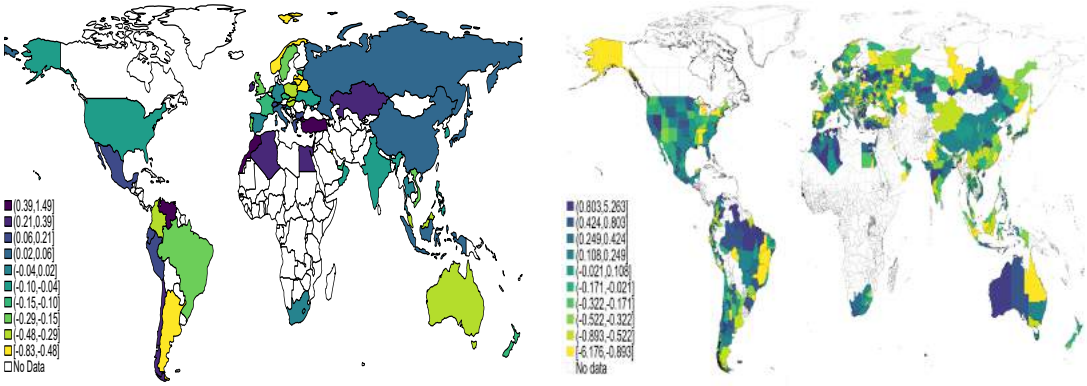

Notes: These maps show log changes in capacity between the current risk landscape, where 10-year floods occur with 10% probability and 100-year floods have a 1% probability, and the projected probabilities for SSP5-8.5, at the country-level in Panel (a) and at the GAUL1-level in Panel (b). Capacities are averaged across 100 simulations of the structural errors. The estimates used to simulate the model are in Table D.2. The probability projections used come from a multimodel ensemble for SSP5-8.5 from the Climate Change Knowledge Portal of the World Bank. The administrative units in the map correspond to GAUL1 units.

change in consumer surplus derived from automobile consumption. In this map, I plot the log change in the price index in the baseline relative to the price index when extreme weather event probabilities in SSP5-8.5. Industry price indices increase in all countries; for the average country, the rise is 2.6%, but there is heterogeneity across different markets.

These price indices increase for three reasons. First, since the main counterfactual essentially constitutes a negative productivity shock becoming more likely, firms shrink in size. This reduces the number of cars that people can consume. Second, firms relocate their production sites from locations that are ex-ante optimal to places that are ex-ante suboptimal causing a decline in productivity. Third, the greater frequency of disasters exacerbates the decline in expected productivity, which in turn results in higher consumer prices.

Figure 9: Log Change in the Price Index for SSP5-8.5

(a) With Firm-Level Adaptation

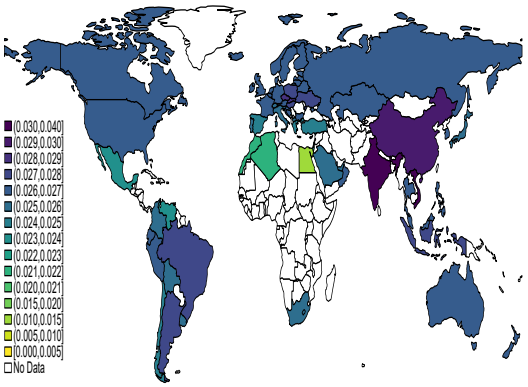

(b) Without Firm-Level Adaptation

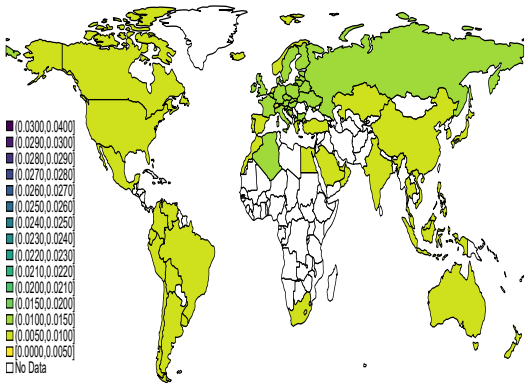

Notes: These maps show log changes in price indices defined by the formula in Equation 4 between the current risk landscape, where 10-year floods occur with 10% probability and 100-year floods have a 1% probability, and the projected probabilities for SSP5-8.5, when firms adapt to the new extreme precipitation probabilities in Panel (a) and when firms' choices are fixed to the ones in the baseline in Panel (b). Price indices are averaged across 100 simulations of the structural errors. The estimates used to simulate the model are in Table D.2. The probability projections used come from a multimodel ensemble for SSP5-8.5 from the Climate Change Knowledge Portal of the World Bank. The administrative units in the map correspond to GAUL1 units.

The fact that production is becoming more costly can be seen in Figure 10. In Panel (a), I show the average increase in marginal costs by country. In most countries, production costs increase. In fact, the average marginal cost, weighted by quantities produced, changes by 7.4%. Nonetheless, in some countries there is a decrease in costs mostly driven by the reallocation of productive firms to locations within those countries. In Panel (b), I show the change in average costs of capacity. On aggregate, capacity costs barely change.

In Figure 11, I decompose the increase in price indices into two components. The first component corresponds to the indirect productivity loss caused by the reallocation of

Figure 10: Log Change in Marginal Costs and Capacity Costs in SSP5-8.5

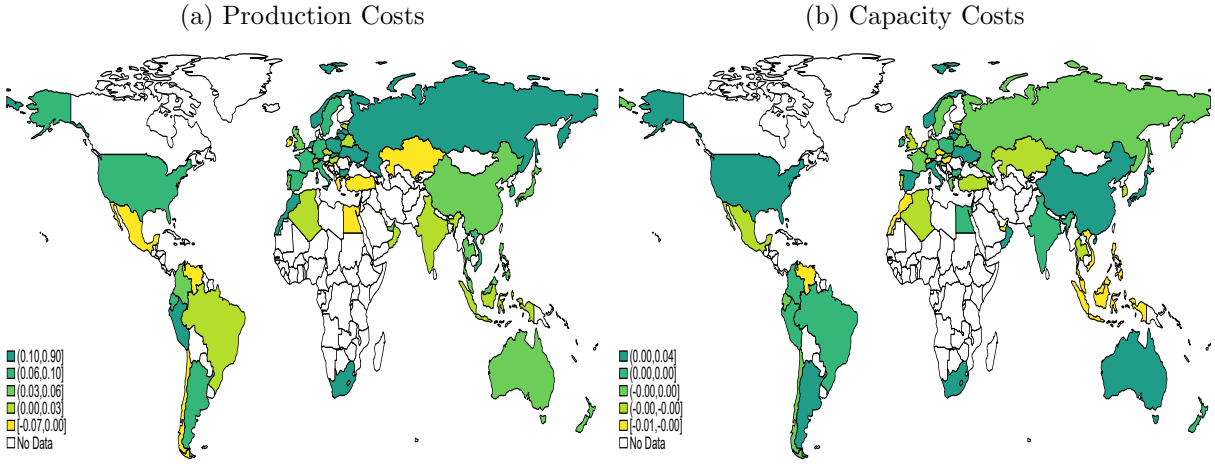

Notes: These maps show log changes in marginal production costs in Panel (a) and capacity costs in Panel (b) between the current risk landscape, where 10-year floods occur with 10% probability and 100-year floods have a 1% probability, and the projected probabilities for SSP5-8.5. In both cases, the country average is constructed as an average across the locations within the country weighted by the quantities produced in each location. Costs are also averaged across 100 simulations of the structural errors. The estimates used to simulate the model are in Table D.2. The probability projections used come from a multimodel ensemble for SSP5-8.5 from the Climate Change Knowledge Portal of the World Bank. The administrative units in the map correspond to GAUL1 units.

production to ex-ante suboptimal locations and the reduction in capacity. The second term corresponds to the direct effect of weather disasters on productivity. I use the following decomposition,

$$\frac{P_j^{'}}{P_j^{o}} = \frac{P_j^{',ns}}{P_j^{o}} \frac{P_j^{'}}{P_j^{',ns}},$$

where $P_j^{'}$ corresponds to the price index in country j after both the shocks become more likely and the plant configurations adapted as a result of the shock to the expectations, P_j^{o} is the value of the price index in country j at the baseline and $P_j^{',ns}$ is the ideal price index in country j when the firms' production organization has been adjusted in response to the change in probabilities, but the frequency of weather events are held at the baseline values. The first term corresponds to the effect of the change in the production structure and the second term to the effects of the shocks, conditional on the plant configuration. As seen in these figures, the main driver of the increase in price indices is the firm-level responses to climate change, rather than the direct impact of the weather shocks.

Finally, I evaluate the effect of firm adaptation on the surplus that consumers derive from the automotive industry. From comparing Figures 9a with 9b, it is clear that prices indices are higher, and the negative effect on consumer surplus is larger, when firms opti-

Figure 11: Decomposing the Effect in Consumer Prices
(Log Change)

(a) Indirect Effect of Reorganization (b) Direct Effect of Weather Disasters

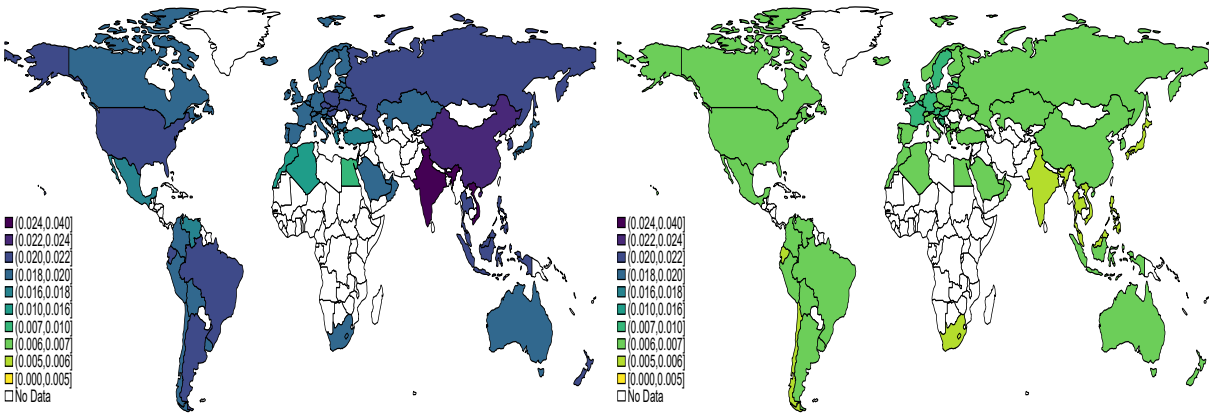

Notes: These maps show a decomposition of log changes in the price indices defined by the formula in Equation 4 between the current risk landscape, where 10-year floods occur with 10% probability and 100-year floods have a 1% probability, and the projected probabilities for SSP5-8.5, in an indirect effect coming from the spatial reorganization of production in Panel (a) and a direct effect of weather disruptions in Panel (b). Price indices are averaged across 100 simulations of the structural errors. The estimates used to simulate the model are in Table D.2. The probability projections used come from a multimodel ensemble for SSP5-8.5 from the Climate Change Knowledge Portal of the World Bank. The administrative units in the map correspond to GAUL1 units.

mally respond to climate change than when they do not.[33] Thus, in this model, firm-level responses to climate change make consumers worse off. The reason for this is that, from the consumers' perspective, productivity shocks to individual firms are not very costly. There are many varieties and when the price of an individual variety increases due to an idiosyncratic disruption, consumers can substitute away to other products without generating a big impact on their welfare. This acts as a very efficient insurance mechanism for consumers. In contrast, firms have an inefficient technology to insure against weather shocks. Firms, on average, have a handful of plants, and creating new plants is costly. A disruption to one of these plants affects their surplus massively. When firms reallocate, aggregate productivity declines considerably as shown in Figure 11. From the perspective of the consumers, the relocation of plants across space is an aggregate shock. With firm-level adaptation, all varieties become, on average, more expensive due to the losses in productivity and capacity. This translates to an aggregate increase in automobile prices for consumers.

[33] In fact, a back-of-the-envelope calculation in which I convert these changes in the price indices to dollar values, suggest a decline of 2,489M in aggregate consumer surplus when firms adapt, but a 915M decline when firms do not adapt. Adding these numbers with the aggregate change in profits, these calculations suggest that total welfare decline by 52,751M when firms adapt, and by 66,858M when firms do not adapt.

5.3 Robustness

I evaluate the sensitivity of the results presented above to alternative values for the impact of floods on car production, and to allowing for spatial correlation in the realization of those floods. In Table 3, I reproduce the main results in Tables 1 and 2 for different values of κ_1 and κ_2, and for different spatial correlation patterns, which are modeled as a function of the distance between two locations with an exponential decay.

In Columns (4) to (7), I consider different values of κ_1 and κ_2. I compare the baseline results to two alternative values for the productivity decline caused by floods. In the first case, floods are twice more damaging than estimated; 10-year floods decrease productivity by 80% and 100-year floods by 90%. In the second case, floods are half as damaging, meaning that 10-year floods decrease productivity by 20% and 100-year floods by 65%. As floods become less damaging, firms have fewer incentives to create more plants and spread out their production to gain resiliency at the expense of productivity. For large weather disasters, the productivity decline is such that firms need to build additional plants to reallocate the affected production. These results also reflect that investments in other types of technologies that reduce the local impact of disasters might be beneficial in addressing the effects of climate change.

Table 3: Firms' Plant Structure and Adaptation - Robustness

Extreme Precipitation Probability	**1%/10%**	**SSP5-8.5**	**1%/10%**	**SSP5-8.5**	**1%/10%**	**SSP5-8.5**	**1%/10%**	**SSP5-8.5**	**1%/10%**	**SSP5-8.5**
Modification	Baseline		$\kappa_1 = 0.11, \kappa_2 = 0.21$		$\kappa_1 = 0.44, \kappa_2 = 0.83$		$\lambda = 0.1$		$\lambda = 0.02$	
Average Locations	6.49	6.78	6.33	6.62	6.53	6.42	6.52	6.78	6.38	6.60
Average Capacity per Firm	465.52	442.92	472.33	452.94	496.97	487.30	462.57	439.29	462.23	437.82
Average Capacity per Plant	152.93	141.91	128.89	116.60	193.06	185.64	147.37	132.58	155.80	135.76
Average Profits	8564.81	8214.25	8442.87	8054.86	9053.46	8934.81	8527.50	8177.72	8391.28	8160.24
Percentage Change in Profits		-4.09%		-4.60%		-1.31%		-4.10%		-2.75%
Average Used Capacity	95.3%	93.0%	92.9%	89.2%	99.6%	99.3%	95.3%	93.2%	94.9%	93.1%
Share of Losses Averted with Adaptation		22.9%		27.3%		9.4%		23.6%		49.91%

Notes: This table computes selected statistics from Tables 1 and 2 with different productivity penalties and correlation structures. Columns (2) and (3) correspond to the baseline results to facilitate comparison. Columns (4) and (5) consider cases in which the productivity declines are larger. Columns (6) and (7) consider cases in which the productivity declines are smaller. Columns (8)-(11) consider two cases in which the spatial correlation in the shocks decays at different rates. Simulation draws are held constant across exercises. The differences solely come from differences in the parameters.

In Columns (8) to (11), I allow for spatial correlation in the realization of extreme weather events. I explore two scenarios, one in which the decay is high, so that the correlation between two locations 300km apart is 0.05 and 1300km away are 0.05 and 0.00, respectively. On the other, the decay is slow, with the correlation for places 300km apart equaling 0.55 and 1300km apart being 0.07.[34] The findings suggest that the incentives

[34] I provide additional details in Appendix F.1.

to adapt the firm's spatial production organization are larger when the potential extreme weather events are spatially correlated.

6 Conclusion

This paper examines how firms adjust to increasing disruptive weather risks due to climate change, focusing on their spatial organization of production through changes in their plants' location, number, and capacity. Using historical data, I document that severe floods significantly disrupt car production in nearby plants. Firms offset part of the output decline by ramping up production at other plants within their network. A model is developed to represent how firms determine their plant locations and capacities, conditional on weather-related disruption risk. I estimate it to match the current car production geography and combine it with climate model projections to simulate counterfactuals where different probabilities of extreme weather events affect the spatial distribution of production.

In the counterfactual analysis, I show that firms build more, albeit smaller, plants in response to climate change. These plants also maintain a larger spare capacity to buffer against weather-induced disruptions. Such adjustments reduce the impact of climate change on firms, decreasing profit losses by one-fifth. However, adaptation adversely affects consumer surplus as plant reconfiguration increases average prices due to productivity and capacity losses. This finding provides a cautionary note for policies incentivizing resilience and managing disruption risks.

Finally, the methodological tools developed in this paper can be adapted to investigate other uncertainty sources such as trade wars, transportation disruption-induced trade costs, labor strike-induced wage changes, or country-specific regulation impacts on multinational activity. Furthermore, the optimization approach can be beneficial in alternative contexts like international trade models with increasing marginal costs or supply chains, and optimal infrastructure models.

References

Alfaro-Ureña, Alonso, Juanma Castro-Vincenzi, Sebastian Fanelli, and Eduardo Morales (2024): "Firm Dynamics with Interdependent Markets," *mimeo*. [5]

Anderson, James E. and Eric van Wincoop (2004): "Trade Costs," *Journal of Economic Literature*, 42 (3), 691–751. [19]

Anderson, Simon P., André de Palma, and Jacques-François Thisse (1988): "The

CES and the logit: Two related models of heterogeneity," *Regional Science and Urban Economics*, 18 (1), 155–164. [12]

Antràs, Pol, Teresa Fort, and Felix Tintelnot (2017): "The Margins of Global Sourcing: Theory and Evidence from U.S. Firms," *American Economic Review*, 107 (9), 2514–2564. [5]

Antràs, Pol, Evgenii Fadeev, Teresa Fort, and Felix Tintelnot (2022): "Global Sourcing and Multinational Activity: A Unified Approach," *Mimeo.* [5]

Arkolakis, Costas, Fabian Eckert, and Rowan Shi (2023): "Combinatorial Discrete Choice: A Quantitative Model of Multinational Location Decisions," *mimeo.* [5]

Arkolakis, Costas, Natalia Ramondo, Andrés Rodríguez-Clare, and Stephen Yeaple (2018): "Innovation and Production in the Global Economy," *American Economic Review*, 108 (8), 2128–73. [5]

Atkin, David and Dave Donaldson (2015): ""Who's Getting Globalized? The Size and Implications of Intra-national Trade Costs"," *Mimeo.* [19]

Balboni, Clare (2021): "In Harm's Way? Infrastructure Investments and the Persistence of Coastal Cities," *Mimeo.* [4]

Balboni, Clare, Johannes Boehm, and Mazhar Waseem (2023): "Firm Adaptation and Production Networks: Structural Evidence from Extreme Weather Events in Pakistan," . [4]

Balinski, M. L. and W. J. Baumol (1968): "The Dual in Nonlinear Programming and Its Economic Interpretation," *The Review of Economic Studies*, 35 (3), 237–256. [16, 17]

Barrot, Jean-Noël and Julien Sauvagnat (2016): " Input Specificity and the Propagation of Idiosyncratic Shocks in Production Networks *," *The Quarterly Journal of Economics*, 131 (3), 1543–1592. [5]

Bates, Paul D., Niall Quinn, Christopher Sampson, Andrew Smith, Oliver Wing, et al. (2021): "Combined Modeling of US Fluvial, Pluvial, and Coastal Flood Hazard Under Current and Future Climates," *Water Resources Research*, 57 (2), e2020WR028673, e2020WR028673 2020WR028673. [2]

Bezanson, Jeff, Alan Edelman, Stefan Karpinski, and Viral B Shah (2017): "Julia: A fresh approach to numerical computing," *SIAM Review*, 59 (1), 65–98. [17]

Bilal, Adrien and Esteban Rossi-Hansberg (2023): "Anticipating Climate Change Across the United States," Working Paper 31323, National Bureau of Economic Research. [4]

Boehm, Christoph E., Aaron Flaaen, and Nitya Pandalai-Nayar (2019): "Input Linkages and the Transmission of Shocks: Firm-Level Evidence from the 2011 Tōhoku Earthquake," *The Review of Economics and Statistics*, 101 (1), 60–75. [5]

Boyd, Stephen and Lieven Vandenberghe (2004): *"Convex Optimization"*, Cambridge University Press. [16, 53]

Brakenridge, GR (2016): "Global active archive of large flood events, Dartmouth Flood Observatory, University of Colorado," *Boulder, CO: Univ. of Colorado.* [-]

Carvalho, Vasco M, Makoto Nirei, Yukiko U Saito, and Alireza Tahbaz-Salehi (2020): "Supply Chain Disruptions: Evidence from the Great East Japan Earthquake*," *The Quarterly Journal of Economics*, 136 (2), 1255–1321. [5]

Castro-Vincenzi, Juanma, Gaurav Khanna, Nicolas Morales, and Nitya Pandalai-Nayar (2024a): "Weathering the Storm: Supply Chains and Climate Risk," Tech. rep., Mimeo. [4]

Castro-Vincenzi, Juanma, Eugenia Menaguale, Eduardo Morales, and Alejandro Sabal (2024b): "Differences in Product Availability Across Countries: Determinants and Welfare Consequences," *mimeo.* [5]

CDP-BMW (2021): "BMW AG CDP Climate Change Questionnaire 2021," Report, Carbon Disclosure Project. [1]

Coşar, Kerem A., Paul L. E. Grieco, Shengyu Li, and Felix Tintelnot (2016): "What Drives Home Market Advantage?" *Journal of International Economics*, 110, 135–150. [6, 20]

Cruz, José-Luis and Esteban Rossi-Hansberg (2023): "The Economic Geography of Global Warming," Tech. rep. [4]

de Chaisemartin, Clément and Xavier D'Haultfoeuille (2022a): "Difference-in-Differences Estimators of Intertemporal Treatment Effects," Working Paper 29873, National Bureau of Economic Research. [7, 9]

——— (2022b): "Two-way Fixed Effects and Differences-in-Differences Estimators with Several Treatments," Tech. rep., Mimeo. [10, 49]

Desmet, Klaus, Robert E. Kopp, Scott A. Kulp, Dávid Krisztián Nagy, Michael Oppenheimer, Esteban Rossi-Hansberg, and Benjamin H. Strauss (2021): "Evaluating the Economic Cost of Coastal Flooding," *American Economic Journal: Macroeconomics*, 13 (2), 444–86. [4]

Dixit, Avinash K and Robert S Pindyck (1994): *Investment under uncertainty*, Princeton university press. [5]

Donaldson, Dave (2018): "Railroads of the Raj: Estimating the Impact of Transportation Infrastructure," *American Economic Review*, 108 (4-5), 899–934. [19]

Ellison, Glenn and Edward L. Glaeser (1997): "Geographic Concentration in U.S. Manufacturing Industries: A Dartboard Approach," *Journal of Political Economy*, 105 (5), 889–927. [2]

Gourieroux, C., A. Monfort, and E. Renault (1993): "Indirect Inference," *Journal of Applied Econometrics*, 8, S85–S118. [21, 22, 58]

Grossman, Gene, Elhanan Helpman, and Hugo Lhuillier (2023a): "Supply Chain Resilience: Should Policy Promote Diversification or Reshoring?" *Journal of Political Economy*. [5]

Grossman, Gene, Elhanan Helpman, and Alejandro Sabal (2023b): "Resilience in Vertical Supply Chains," *Mimeo*. [5]

Gu, Grace and Galina Hale (2022): "Climate Risks and FDI," *Mimeo*. [4]

Head, Keith and Thierry Mayer (2019): "Brands in Motion: How Frictions Shape Multinational Production," *American Economic Review*, 109 (9), 3073–3124. [5, 6, 20]

Head, Keith, Thierry Mayer, and Marc Melitz (2024): "The unintended consequences of high regional content requirements," in *Local Content Requirements: Promises and Pitfalls*, ed. by Lili Yan Ing and Gene M. Grossman, New York: Routledge. [2]

Helpman, Elhanan, Marc J. Melitz, and Stephen R. Yeaple (2004): "Export Versus FDI with Heterogeneous Firms," *American Economic Review*, 94 (1), 300–316. [2, 5, 11]

Hirabayashi, Yukiko, Masahiro Tanoue, Orie Sasaki, Xudong Zhou, and Dai Yamazaki (2021): "Global exposure to flooding from the new CMIP6 climate model projections," *Scientific Reports*, 11 (1), 3740. [2]

Hsiao, Allan (2023): "Sea Level Rise and Urban Adaptation in Jakarta," *Mimeo.* [4]

Indaco, Agustín, Francesc Ortega, Taspinar, and Süleyman (2020): "Hurricanes, flood risk and the economic adaptation of businesses," *Journal of Economic Geography*, 21 (4), 557–591. [4]

IPCC (2021a): *Climate Change 2021: The Physical Science Basis. Contribution of Working Group I to the Sixth Assessment Report of the Intergovernmental Panel on Climate Change*, vol. In Press, Cambridge, United Kingdom and New York, NY, USA: Cambridge University Press. [1, 2, 26]

——— (2021b): *Summary for Policymakers*, Cambridge, United Kingdom and New York, NY, USA: Cambridge University Press, 332. [26]

ITC (2022): "Market Access Map," . [18]

Jia, Ruixue, Xiao Ma, and Victoria Wenxin Xie (2022): "Expecting Floods: Firm Entry, Employment, and Aggregate Implications," Working Paper 30250, National Bureau of Economic Research. [4]

Jiang, Bomin, Daniel E Rigobon, and Roberto Rigobon (2021): "From Just in Time, to Just in Case, to Just in Worst-Case: Simple models of a Global Supply Chain under Uncertain Aggregate Shocks." Working Paper 29345, National Bureau of Economic Research. [5]

Klier, Thomas and James Rubenstein (2008): *Who Really Made Your Car? Restructuring and Geographic change in the Auto Industry*, no. wrmyc in Books from Upjohn Press, W.E. Upjohn Institute for Employment Research. [2]

Kopytov, A., B. Mishra, K. Nimark, and M. Taschereau-Dumouchel (2023): "Endogenous Production Networks under Supply Chain Uncertainty," *mimeo.* [5]

Kummu, Matti, Maija Taka, and Joseph H. A. Guillaume (2018): "Gridded global datasets for Gross Domestic Product and Human Development Index over 1990–2015," *Scientific Data*, 5 (1), 180004. [18, 46]

Legat, Benoît, Oscar Dowson, Joaquim Dias Garcia, and Miles Lubin (2021): "MathOptInterface: a data structure for mathematical optimization problems," *INFORMS Journal on Computing*. [55]

Letchford, Adam N. and Andrew J. Parkes (2018): "A guide to conic optimisation and its applications," *RAIRO-Oper. Res.*, 52 (4). [17]

Li, Zhi, Shang Gao, Mengye Chen, Jonathan J. Gourley, Changhai Liu, Andreas F. Prein, and Yang Hong (2022): "The conterminous United States are projected to become more prone to flash floods in a high-end emissions scenario," *Communications Earth & Environment*, 3 (1), 86. [2]

Lloyd, Christopher T., Heather Chamberlain, David Kerr, Greg Yetman, Linda Pistolesi, Forrest R. Stevens, Andrea E. Gaughan, Jeremiah J. Nieves, Graeme Hornby, Kytt MacManus, Parmanand Sinha, Maksym Bondarenko, Alessandro Sorichetta, and Andrew J. Tatem (2019): "Global spatio-temporally harmonised datasets for producing high-resolution gridded population distribution datasets," *Big Earth Data*, 3 (2), 108–139, pMID: 31565697. [46]

Lubin, Miles, Oscar Dowson, Joaquim Dias Garcia, Joey Huchette, Benoît Legat, and Juan Pablo Vielma (2023): "JuMP 1.0: Recent improvements to a modeling language for mathematical optimization," *Mathematical Programming Computation*. [17]

Markus, Frank (2021): "What, Exactly, Is an Automotive Platform?" *Motor Trend*. [10]

Mayer, Thierry and Soledad Zignago (2011): "Notes on CEPII's Distances Measures: the GeoDist Database," *CEPII Working Paper*, 2011-25. [18]

Meijer, Johan R, Mark A J Huijbregts, Kees C G J Schotten, and Aafke M Schipper (2018): "Global patterns of current and future road infrastructure," *Environmental Research Letters*, 13 (6), 064006. [18, 46]

MOSEK ApS (2022): *MOSEK Optimization Suite*. [17]

——— (2023): *MOSEK Modeling Cookbook*. [17]

Nath, Ishan. (2022): ""Climate Change, The Food Problem, and the Challenge of Adaptation through Sectoral Reallocation"," *Mimeo*. [4]

Pankratz, Nora and Christoph Schiller (2021): "Climate Change and Adaptation in Global Supply-Chain Networks," *Mimeo.* [4]

Pindyck, Robert S. (1988): "Irreversible Investment, Capacity Choice, and the Value of the Firm," *The American Economic Review*, 78 (5), 969–985. [5]

——— (1993): "A Note on Competitive Investment under Uncertainty," *The American Economic Review*, 83 (1), 273–277. [5]

Ramondo, Natalia (2014): "A quantitative approach to multinational production," *Journal of International Economics*, 93 (1), 108–122. [5]

Ramondo, Natalia, Veronica Rappoport, and Kim J. Ruhl (2013): "The Proximity-Concentration Tradeoff under Uncertainty," *The Review of Economic Studies*, 80 (4), 1582–1621. [5]

Ramondo, Natalia and Andrés Rodríguez-Clare (2013): "Trade, Multinational Production, and the Gains from Openness," *Journal of Political Economy*, 121 (2), 273–322. [5]

Rob, Rafael and Nikolaos Vettas (2003): "Foreign Direct Investment and Exports with Growing Demand," *The Review of Economic Studies*, 70 (3), 629–648. [5]

Saiz, A. (2010): "The Geographic Determinants of Housing Supply," *Quartely Journal of Economics*, 125(3), 1253–1296. [18]

Tintelnot, Felix (2017): "Global Production with Export Platforms*," *The Quarterly Journal of Economics*, 132 (1), 157–209. [2, 5, 11]

Wolfe, Philip (1961): "A Duality Theorem for Non-Linear Programming," *Quarterly of Applied Mathematics*, 19 (3), 239–244. [52]

World Meteorological Organization (2022): "State of Global Water Resources Report 2022," Tech. rep., World Meteorological Organization. [2]

WorldPop (2021): *The Spatial Distribution of Population in 2020.* [18, 46]

Zanaga, Daniele, Ruben Van De Kerchove, Wanda De Keersmaecker, Niels Souverijns, et al. (2021): "ESA WorldCover 10 m 2020 v100," . [18, 47]

ONLINE APPENDIX

A Anecdotal Evidence

A.1 Anecdotal Evidence of Weather Disruptions to Car Production

1. *Hurricane Ian forces Mercedes, Volvo to shutter S.C. plants after blasting Florida*, Automotive News, September 29, 2022
2. *Typhoon Hinnamoor halts production in Japan and South Korea*, Automotive Logistics, September 06, 2022
3. *Factory closures extended in China as drought continues*, Automotive Logistics, August 17, 2022
4. *Heavy rains hit Toyota production in Japan*, Automotive Logistics, August 02, 2022
5. *Floods hit auto production and supply in South Africa*, Automotive Logistics, May 30, 2022
6. *Drowned vehicles, stuck workers: Jeep, Ford plants halted amid Detroit flooding*, Detroit Free Press, June 30, 2021
7. *Texas winter storm blackouts hit automotive sector*, Automotive Logistics, February 22, 2022
8. *GM to reopen Corvette plant after Ky. tornado*, Automotive News, December 17, 2021
9. *US tornado damage hits production and logistics*, Automotive Logistics, December 13, 2021
10. *Typhoon forces Subaru to halt production at Gunma*, Automotive Logistics, October 22, 2019
11. *Subaru halts production for 10 days after Typhoon Hagibis*, Nikkei Asia, October 17, 2019
12. *Auto industry still assessing impact of hurricane*, Automotive Logistics, September 19, 2018
13. *Mazda loses 44,000 units of output in Japan due to torrential rains*, Automotive News Europe, September 21, 2018
14. *Auto Industry anticipates production losses ahead of Hurricane Florence*, Freight Waves, September 12, 2018
15. *Japanese carmakers count the cost of natural disasters*, Automotive Logistics, September 11, 2018
16. *Toyota shuts South African plant after 'significant damage' from flooding*, Automotive Logistics, October 11, 2017
17. *Storm damage halts Toyota production in Durban*, Motorpress, October 10, 2017
18. *Hyundai and Kia Are Temporarily Closing Plants in Path of Irma*, The Drive, September 11, 2017
19. *OEMs and logistics providers assess damage from Hurricane Harvey*, The Drive, September 4, 2017
20. *FCA Minivan Production resumes as in Ontario as flood water recedes*, The Drive, August 29, 2017
21. *Limited damage to vehicles after surprise hailstorm in Valencia*, Automotive Logistics, December 12, 2017
22. *Audi using emergency measures to deal with floods at Neckarsulm*, Automotive Logistics, June 1, 2016
23. *Audi production in Germany hit by flooding*, Automotive News Europe, May 30, 2016
24. *Storm halts Toyota production in Texas*, Automotive Logistics, May 19, 2016

25. *Renewed flooding hits carmakers in India*, Automotive Logistics, December 2, 2015

26. *Hyundai, Ford, Renault suspend operations in Chennai due to floods*, Economic Times, December 02, 2015

27. *Flooding in Chennai causes plant closures and supply disruption*, Automotive Logistics, November 18, 2015

28. *Detroit, Which Now Looks More Like Venice, Is So Flooded That Factories Have Been Affected*, Bangshift.com, August 13, 2014

29. *Porsche stops Cayenne and Panamera production as floods hit supplies*, Automotive News, July 6, 2013

30. *Thai floods affect Honda's Global Output*, Automotive Logistics, November 1, 2011

31. *Thailand floods stall automakers*, CNN Money, October 28, 2011

32. *Tornado Damage Closes Mercedes-Benz Alabama Plant*, Motortrend, April 28, 2011

33. *Guangzhou Honda's engine supplier hit hard by floods*, Automotive News, June 18, 2008

34. *Heatwave forces PSA Peugeot Citroen to trim output*, Automotive News, August 12, 2003

35. *Fiat says Feb Italy Mkt Share 27.5 pct after Floods*, Wards Auto, March 03, 2003

36. *Flooding Forces PSA to Shut 5 Plants*, Automotive News, February 6, 1995

Figure A.1: The impact of flooding in Honda's Celaya plant

(a) Honda's Celaya Plant after Flood

(b) Location of Honda's Plants in Mexico

(c) Production in Celaya Plant

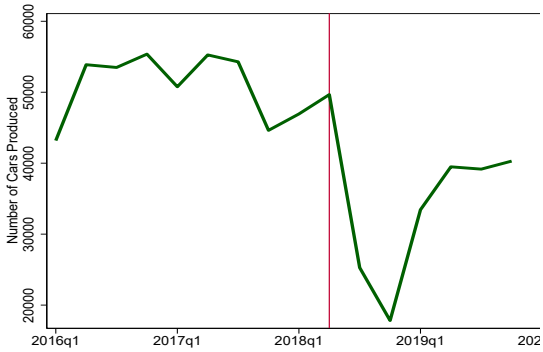

(d) Production in El Salto Plant

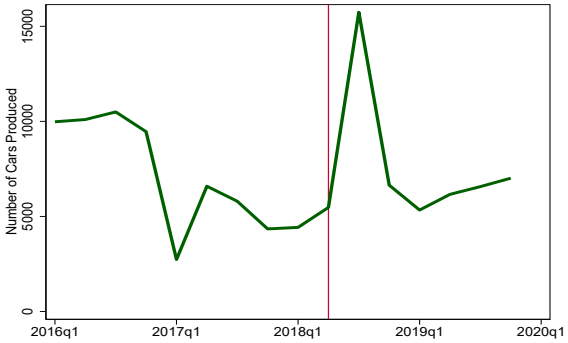

Notes: The source of the photograph in Panel (a) is Automotive News. It shows the flooded Honda plant in Celaya, Mexico. Panel (b) shows a map of Mexico with the location of Honda's plants. Panels (c) and (d) shows production in the Celaya and El Salto plants around the flooding event.

A.2 Data Appendix

A.2.1 Global Car Data

Figure A.2: Data - Location of Production and of Plants

(a) Number of Produced Units (b) Number of Plants

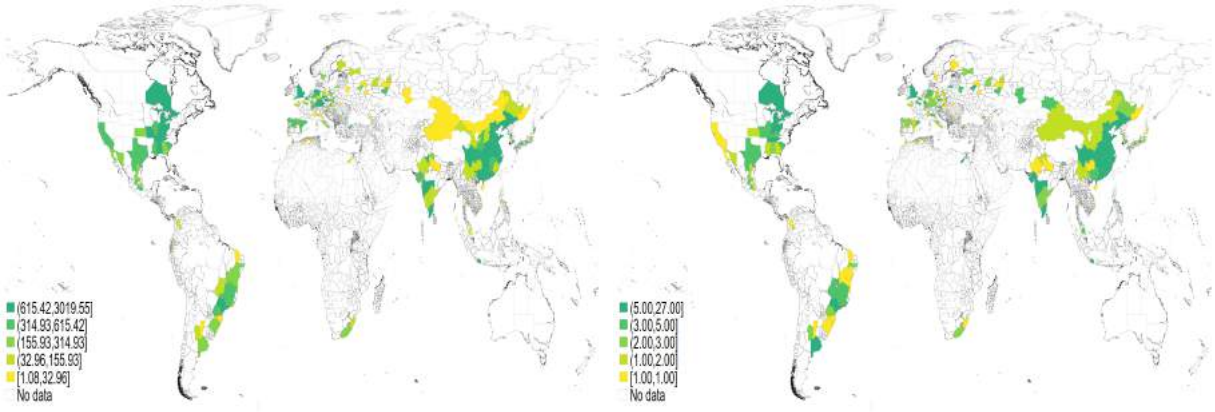

Notes: These maps show the number of cars (in thousands) and the number of plants in 2019. The locations taken into account correspond to the GAUL1 units where there is car production in 2019.

Figure A.3: Locations Included in the Estimation

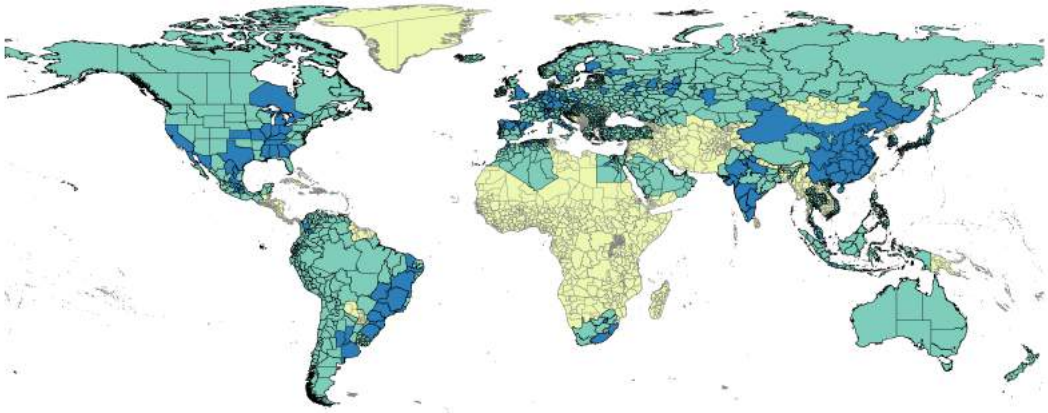

Notes: Regions in blue are included in the estimation of the model. These are the regions where at least one plant is located in 2019 in the car registration dataset. Additionally, regions in green are included in the counterfactuals of the model. These are regions in the countries with sales in the car registration dataset. The other regions are not included in either the estimation or the counterfactuals. The administrative units correspond to GAUL1 units.

A.2.2 Location-Specific Variables

Local Population

I source population counts in 2020 for each 1km grid from the WorldPop project (WorldPop 2021).[35] The high-resolution projections of the distribution of population around the world follow the methods presented in Lloyd et al. (2019). I convert the population counts for 1km grids to population counts at the GAUL1 level, by adding up the grids within the borders of each unit. For grids located in multiple GAUL1 units, population counts are apportioned proportionately.

Figure A.4: Local Population (in logs)

(a) All (b) Locations in Counterfactual

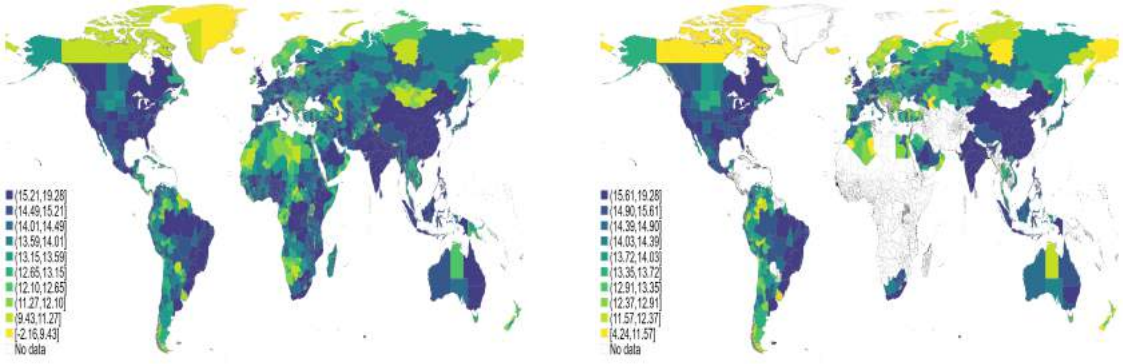

Local Road Density

I construct measures of local road density using data from Meijer et al. (2018).[36] This dataset provides information of global and regional vector datasets in shapefile format, and global raster datasets of road density at a 5 arcminutes resolution. The dataset contains information for different types of roads. To construct my measure of road density, I compute the share of grids that contain primary roads or highways within a GAUL1 unit and compute the simple average.

Local Gross Domestic Product per Capita in PPP

I construct measures of local GDP per capita using data from Kummu et al. (2018).[37] This dataset provides estimates of gross domestic product based on purchasing power parity at a 5 arc-min resolution for 2015. For each GAUL1 unit, I aggregate these estimates to get

[35] This dataset can be downloaded in https://hub.worldpop.org/geodata/listing?id=64.

[36] This dataset can be downloaded in https://www.globio.info/download-grip-dataset.

[37] This dataset can be downloaded in https://datadryad.org/stash/dataset/doi:10.5061/dryad.dk1j0.

Figure A.5: Local Road Density (in logs)

(a) All

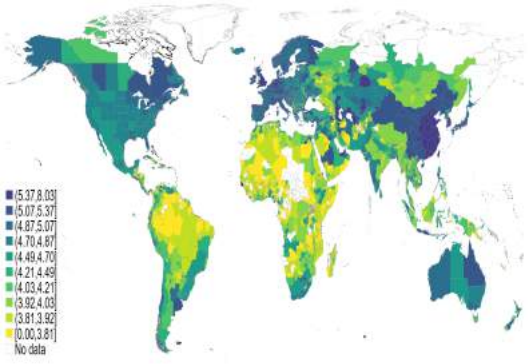

(b) Locations in Counterfactual

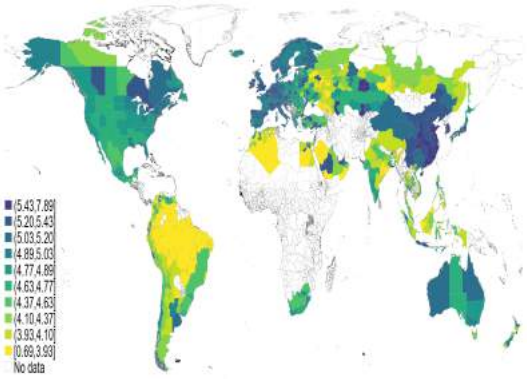

a value for gross domestic production at the GAUL1 level. Then, I divide by the GAUL1 population counts to get a measure of GDP per capita.

Figure A.6: Local Gross Domestic Product per Capita in PPP (in logs)

(a) All

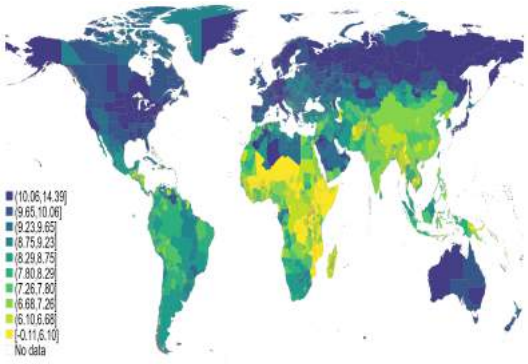

(b) Locations in Counterfactual

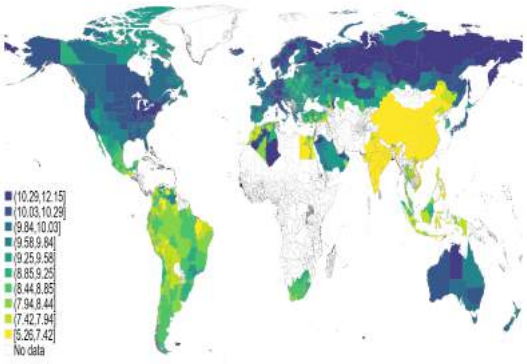

Local Land Availability

I define land availability in a given region as the share of undeveloped land, i.e., excluding buildings, croplands, marshes, glaciers, and deserts, with a slope smaller than 15%. I obtain information about global land use from the WorldCover project of the European Space Agency (Zanaga et al. 2021).[38] For each 10m by 10m pixel, I compute two variables. First, I compute its slope. Second, I compute whether the land is occupied by a building or a permanent crop, or by deserts, marshes or glaciers. For each GAUL1 unit, I compute the share of pixels that have buildable land.

[38]This dataset can be downloaded in https://worldcover2020.esa.int/download.

Figure A.7: Local Land Availability (in Shares)

(a) All

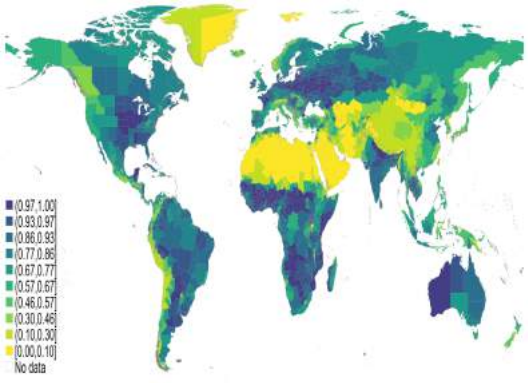

(b) Locations in Counterfactual

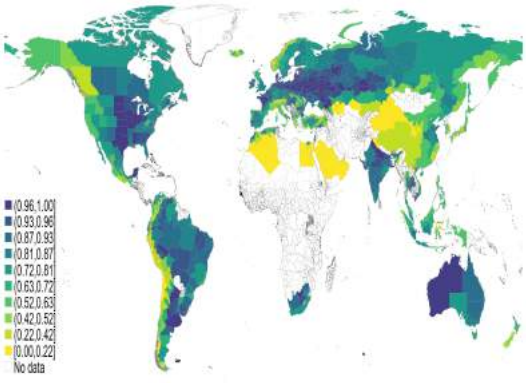

B Additional Reduced Form Exercises

Figure B.1: The Impact of Severe Floods on the Extensive Margin of Plant Location

(a) Probability of Operating

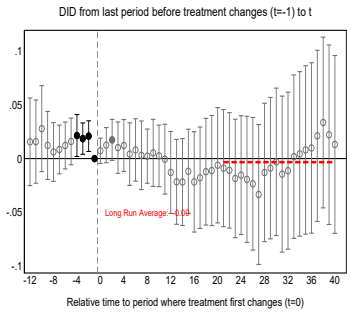

(b) Number of Plants in GAUL2

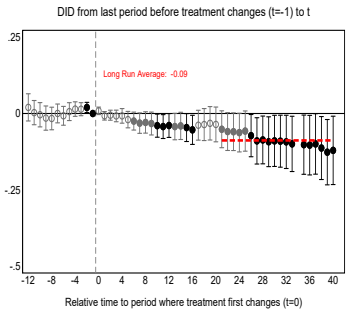

Notes: In these plots, the y-axis shows the values of Equation 1 for the outcome Log Plant Production for 0 to 40 quarters after the plant was flooded for the first time in Panel (a) and Log Number of Plants in a GAUL2 location for 0 to 40 quarters after the location experienced a flood for the first time. The pre-trend estimates are computed using long-difference placebo estimators. The sample comprises production plants that were active in did not experience any flooding events on the 20 quarters before the first period in the sample. Standard errors are clustered at the GAUL1 administrative level and computed with 100 bootstrap replications. The circles correspond to the point estimate, the bars correspond to 95% confidence intervals and the colors of the circle mean ● significant at 5%, ● at 10%, ○ not significant at 10%.

Figure B.2: The Impact of Severe Floods on Car Production - Controlling for Spillovers

(a) All Floods

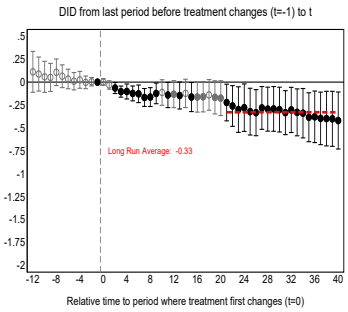

(b) 100-year Floods

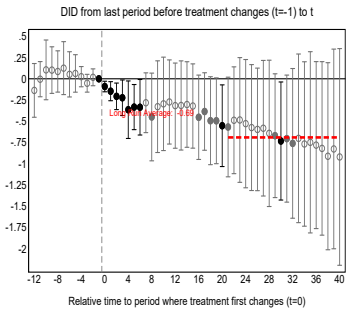

(c) 10-year Floods

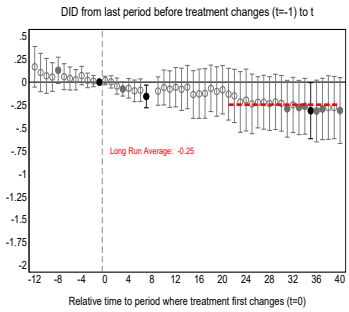

Notes: In these plots, the y-axis shows the values of Equation 1 for the outcome Log Plant Production for 0 to 40 quarters after the plant was flooded for the first time. I account for potential spillovers between plants of the same firm by using the modification proposed in Section 4 of de Chaisemartin and D'Haultfoeuille (2022b). The pre-trend estimates are computed using long-difference placebo estimators. The sample comprises production plants that produce 50 units or more during all the quarters between 2000-2019 and did not experience any flooding events on the 20 quarters before the first period in the sample. Standard errors are clustered at the GAUL1 administrative level and computed with 100 bootstrap replications. The circles correspond to the point estimate, the bars correspond to 95% confidence intervals and the colors of the circle mean ● significant at 5%, ● at 10%, ○ not significant at 10%.

Figure B.3: The Impact of 100-year Floods on Car Production - Alternative Thresholds

Panel A: All Floods

(a) 25 km (b) 50 km (c) 75 km

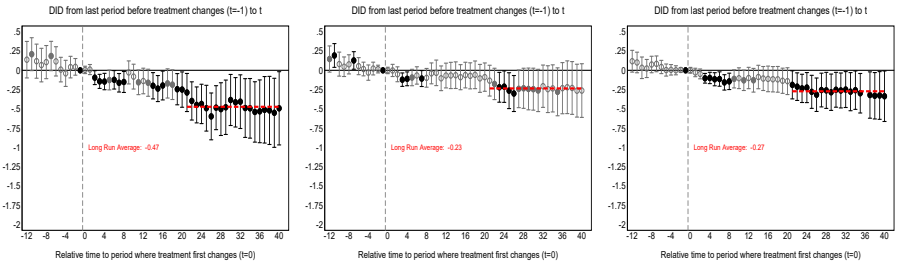

(d) 100 km (e) 150 km (f) 200 km

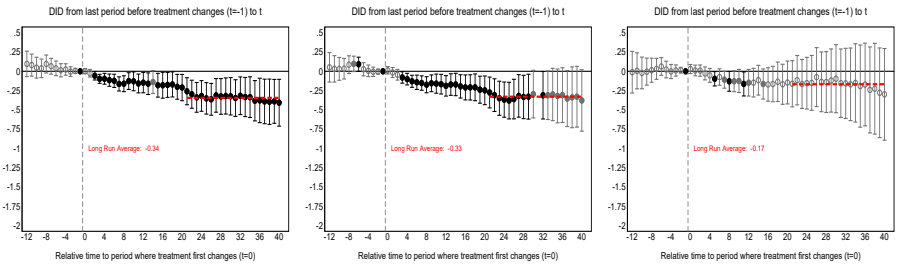

Panel B: 100-Year Floods

(g) 25 km (h) 50 km (i) 75 km

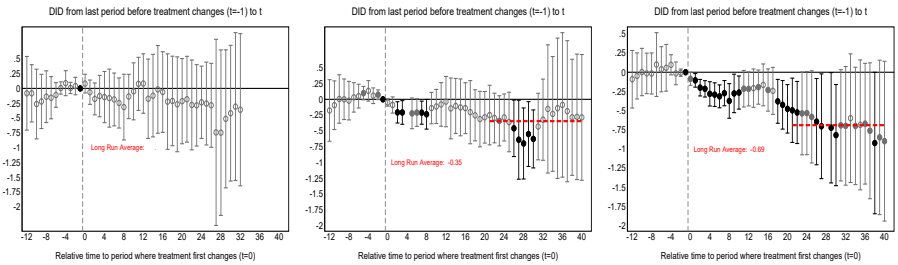

(j) 100 km (k) 150 km (l) 200 km

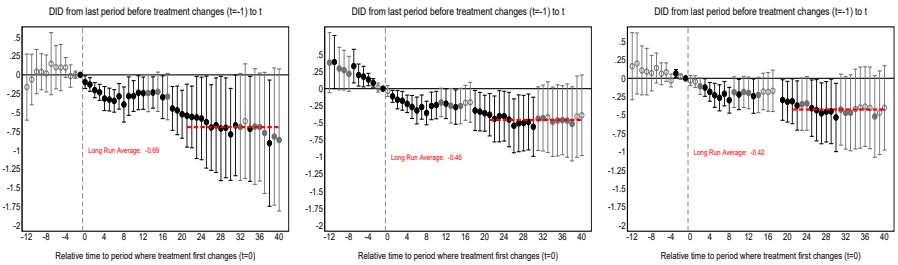

Notes: In these plots, the y-axis shows the values of Equation 1 for the outcome Log Plant Production for 0 to 40 quarters after the plant was flooded for the first time. The pre-trend estimates are computed using long-difference placebo estimators. Floods are defined using different distance thresholds. The sample comprises production plants that produce 50 units or more during all the quarters between 2000-2019 and did not experience any flooding events on the 20 quarters before the first period in the sample. Standard errors are clustered at the GAUL1 administrative level and computed with 100 bootstrap replications. The circles correspond to the point estimate, the bars correspond to 95% confidence intervals and the colors of the circle mean ● significant at 5%, ● at 10%, ○ not significant at 10%.

C Additional Model Details

C.1 Proofs

Proposition 1 *The* ex-ante *capacity choice optimization problem of the firm is a concave objective function defined on a set of linear constraints.*

Proof *Since the capacity investment cost functions are convex and the constraints are conventional (linear) non-negativity constraints, it suffices to show that the expected operating profits function* $\mathbb{E}_{\boldsymbol{\varepsilon_n}}\left[\Pi_n(\boldsymbol{C_n}, \boldsymbol{\varepsilon_n})\right]$ *is concave in the vector* $\boldsymbol{C}$*. The expectation operator preserves the concavity of* $\Pi_n(\boldsymbol{C_n}, \boldsymbol{\varepsilon_n})$ *which is the only thing required to prove.*

Let $\boldsymbol{C'}, \boldsymbol{C''} \in \mathbb{R}_+^I$*, pick an arbitrary vector of productivities* $\boldsymbol{\varepsilon} \in \mathbb{R}_+^I$ *and* $\theta \in (0,1)$*. Define a function* $f(\boldsymbol{q}) = \sum_{j=1}^J \beta_{jn}\left(\sum_{i=1}^I q_{ij}\right)^{\frac{\sigma-1}{\sigma}} - \sum_{j=1}^J \sum_{i=1}^I \frac{\tau_{ij} w_i}{\varepsilon_{in}} q_{ij}$ *and a convex set* $D(\boldsymbol{C}) = \left\{q_{ij} : \sum_{j=1}^J \tau_{ij} q_{ij} \leqslant C_i,\ \forall i \in I, j \in J\right\}$*. Notice that the function* $f(q)$ *is concave. Let* $q' \equiv \operatorname{argmax}_{q \in D(C')} f(q)$ *and* $q'' \equiv \operatorname{argmax}_{q \in D(C'')} f(q)$*. Then,*

$$\begin{aligned}\Pi(\theta \boldsymbol{C'} + (1-\theta)\boldsymbol{C''}, \boldsymbol{\varepsilon}) \equiv & \max_{q \in D(\theta C' + (1-\theta) C'')} f(q) \geqslant \\ & f(\theta q' + (1-\theta) q'') \geqslant \\ & \theta f(q') + (1-\theta) f(q'') \\ = & \theta \Pi(\boldsymbol{C'}, \boldsymbol{\varepsilon}) + (1-\theta)\Pi(\boldsymbol{C''}, \boldsymbol{\varepsilon}) \square\end{aligned}$$

Proposition 2 *The dual ex-ante optimization problem of firm* n *is*

$$\begin{aligned}&\min_{\nu_{ins} \geqslant 0} \frac{\left(\frac{\sigma-1}{\sigma}\right)^{\sigma-1}}{\sigma} \sum_{s=1}^S \sum_{j=1}^J \frac{\beta_{jn}^\sigma}{S}\left(\min_i\left\{\tau_{ij}\left(\frac{w_i}{\varepsilon_{ins}} + \nu_{ins}\right)\right\}\right)^{1-\sigma} \\ &s.t\ \ \frac{1}{S}\sum_{s=1}^S \nu_{ins} \leqslant \alpha_{in}\ \ \ [C_{in}]\ \ \ \forall i\end{aligned}$$

Proof *Consider the following optimization problem,*

$$\begin{aligned}&\max_{q_{ijns}, C_{in} \geqslant 0}\ \frac{1}{S}\sum_{s=1}^S\left[\sum_{j=1}^J \beta_{jn}\left(\sum_{i=1}^I q_{ijns}\right)^{\frac{\sigma-1}{\sigma}} - \sum_{i=1}^I \sum_{j=1}^J \frac{w_i}{\varepsilon_{ins}} \tau_{ij} q_{ijns}\right] - \sum_{i=1}^{\mathcal{I}} \alpha_{in} C_{in} \\ &s.t\ \ \frac{1}{S}\sum_{j=1}^J \tau_{ij} q_{ijns} \leqslant \frac{1}{S} C_{in}\ \ \forall i, s\ \ \ [\nu_{ins}]\,.\end{aligned}$$

Start from the Lagrangian function of the Problem described above,

$$\mathcal{L} = \frac{1}{S}\left(\sum_{j=1}^{J}\beta_{jn}\left(\sum_{i=1}^{I}q_{ijns}\right)^{\frac{\sigma-1}{\sigma}} - \sum_{j=1}^{J}\sum_{i=1}^{I}\frac{\tau_{ij}w_i}{\varepsilon_{ins}}q_{ijns}\right) - \sum_{i=1}^{\mathcal{I}}\alpha_{in}C_{in} - \frac{1}{S}\sum_{i=1}^{I}\sum_{s=1}^{S}\nu_{ins}\left(\sum_{j=1}^{J}\tau_{ij}q_{ijns} - C_{in}\right).$$

From the definition of the dual function,

$$D(\boldsymbol{\nu}_n) = \max_{q_{ijn},C_{in}\geqslant 0}\frac{1}{S}\left(\sum_{j=1}^{J}\beta_{jn}\left(\sum_{i=1}^{I}q_{ijn}\right)^{\frac{\sigma-1}{\sigma}} - \sum_{j=1}^{J}\sum_{i=1}^{I}\tau_{ij}\left(\frac{w_i}{\varepsilon_{in}}+\nu_{ins}\right)q_{ijn}\right) + \sum_{i=1}^{I}C_{in}\left(\frac{1}{S}\sum_{s=1}^{S}\nu_{ins} - \alpha_{in}\right).$$

The first order condition for an arbitrary q_{ijns} is given by

$$\frac{\sigma-1}{\sigma}\beta_{jn}\left(\sum_{i=1}^{I}q_{ijns}\right)^{-\frac{1}{\sigma}} - \tau_{ij}\left(\frac{w_i}{\varepsilon_{ins}}+\nu_{ins}\right) \leqslant 0$$

Likewise, the first order condition for C_{is} is

$$\frac{1}{S}\sum_{s=1}^{S}\nu_{ins} - \alpha_{in} \leqslant 0.$$

Then, one can write the dual problem based on Wolfe (1961), as

$$\begin{aligned}
\min_{\nu_{ins}\geqslant 0}\ & \frac{1}{S}\frac{\left(\frac{\sigma-1}{\sigma}\right)^{\sigma-1}}{\sigma}\sum_{s=1}^{S}\left[\sum_{j=1}^{J}\beta_{jn}\left(\sum_{i=1}^{I}q_{ijns}\right)^{\frac{\sigma-1}{\sigma}} - \sum_{j=1}^{J}\sum_{i=1}^{I}\tau_{ij}\left(\frac{w_i}{\varepsilon_{ins}}+\nu_{ins}\right)q_{ijns}\right] \\
s.t\ & \frac{\sigma-1}{\sigma}\beta_{jn}\left(\sum_{i=1}^{I}q_{ijns}\right)^{-\frac{1}{\sigma}} - \tau_{ij}\left(\frac{w_i}{\varepsilon_{ins}}+\nu_{ins}\right) \leqslant 0 \quad \forall i,j,s \\
& \frac{1}{S}\sum_{s=1}^{S}\nu_{ins} \leqslant \alpha_{in} \quad \forall i
\end{aligned}$$

This dual optimization problem can be further simplified by introducing the first group of constraints in the objective function. From the first order conditions for q_{ijns}, it must be that

$$Q_{jns} \equiv \left(\sum_{i=1}^{I}q_{ijns}\right) = \beta_{jn}^{\sigma}\left(\frac{\sigma-1}{\sigma}\right)^{\sigma}\left(\min_{i}\left\{\tau_{ij}\left(\frac{w_i}{\varepsilon_{ins}}+\nu_{ins}\right)\right\}\right)^{-\sigma},$$

but also, these imply that

$$\sum_{j=1}^{J}\sum_{i=1}^{I}\tau_{ij}\left(\frac{w_i}{\varepsilon_{ins}}+\nu_{ins}\right)q_{ijns}=\sum_{j=1}^{J}\sum_{i=1}^{I}\frac{\sigma-1}{\sigma}\beta_{jn}Q_{jns}^{-\frac{1}{\sigma}}q_{ijns}=\sum_{j=1}^{J}\frac{\sigma-1}{\sigma}\beta_{jn}Q_{jn}^{-\frac{1}{\sigma}}\underbrace{\sum_{i=1}^{I}q_{ijns}}_{Q_{jns}}$$

Then, replacing this in the dual function, the dual problem of the firm n is given by

$$\min_{\nu_{ins}\geqslant 0}\frac{\left(\frac{\sigma-1}{\sigma}\right)^{\sigma-1}}{\sigma}\sum_{s=1}^{S}\sum_{j=1}^{J}\frac{\beta_{jn}^{\sigma}}{S}\left(\min_{i}\left\{\tau_{ij}\left(\frac{w_i}{\varepsilon_{ins}}+\nu_{ins}\right)\right\}\right)^{1-\sigma}$$

$$s.t\ \ \frac{1}{S}\sum_{s=1}^{S}\nu_{ins}\leqslant\alpha_{in}\ \ \ [C_i]\ \ \ \forall i$$

Proposition 3 *The dual optimization problem described in Proposition 2 can be written as the minimization of a linear objective function on a convex set as*

$$\min_{\nu_{ins},\mu_{jns},t_{jns}\geqslant 0}\frac{\left(\frac{\sigma-1}{\sigma}\right)^{\sigma-1}}{\sigma}\sum_{s=1}^{S}\sum_{j=1}^{J}\frac{\beta_{jn}^{\sigma}}{S}t_{jns}$$

$$s.t\ \ \sum_{s=1}^{S}\frac{\nu_{ins}}{S}\leqslant f'_{in}(C_{in})\ \ \forall i;\ \ \mu_{jns}\leqslant\tau_{ij}\left(\frac{w_i}{\varepsilon_{ins}}+\nu_{ins}\right)\ \ \forall i,j,s;\ \ (t_{jns},\mu_{jns},1)\in P_3^{\frac{1}{\sigma},1-\frac{1}{\sigma}}\ \ \forall j,s$$

Proof *Starting from the problem in Proposition 2, substitute* $\min_i\left\{\tau_{ij}\left(\frac{w_i}{\varepsilon_{ins}}+\nu_{ins}\right)\right\}$ *for a new variable* μ_{js} *for all* $j\in J$ *and* $s\in S$ *and add constraints for all* i,j *and* s *such that* $\mu_{jns}\leqslant\tau_{ij}\left(\frac{w_i}{\varepsilon_{ins}}+\nu_{ins}\right)$*. The problem becomes*

$$\min_{\nu_{ins},\mu_{jns}\geqslant 0}\frac{\left(\frac{\sigma-1}{\sigma}\right)^{\sigma-1}}{\sigma}\sum_{s=1}^{S}\sum_{j=1}^{J}\frac{\beta_{jn}^{\sigma}}{S}\mu_{jns}^{1-\sigma}$$

$$s.t\ \ \frac{1}{S}\sum_{s=1}^{S}\nu_{ins}\leqslant\alpha_{in}\ \ \forall i\,,\ \ \mu_{jns}\leqslant\tau_{ij}\left(\frac{w_i}{\varepsilon_{ins}}+\nu_{ins}\right)\ \ \forall i,j,s$$

To make the problem linear, notice that one can substitute $\mu_{jns}^{1-\sigma}$ *for* t_{jns} *and add power cones as constraints. A three-dimensional power cone is defined as*

$$P_3^{\alpha,1-\alpha}=\left\{x\in\mathbb{R}^3:x_1^{\alpha}x_2^{1-\alpha}\geqslant|x_3|,x_1,x_2\geqslant 0\right\}.$$

I substitute the nonlinear term $\mu_{jns}^{1-\sigma}$ *for a new auxiliary variable* t_{jns} *such that* $t_{jn}\geqslant\mu_{jn}^{1-\sigma}$*. This step consists on writing the problem in the equivalent* epigraph *form (see Boyd and*

Vandenberghe 2004). This nonlinear inequality condition can be formalized using a three-dimensional cone, $(t_{jns}, \mu_{jns}, 1) \in P_3^{\frac{1}{\sigma}, 1-\frac{1}{\sigma}}$. *In the optimum, these two variables will coincide since minimizing the objective function involves choosing the smallest* t_{jns} *or the largest* μ_{jns} *possible. Then, the problem is*

$$\min_{\nu_{ins}, \mu_{jns}, t_{jns} \geqslant 0} \frac{\left(\frac{\sigma-1}{\sigma}\right)^{\sigma-1}}{\sigma} \sum_{s=1}^{S} \sum_{j=1}^{J} \frac{\beta_{jn}^{\sigma}}{S} t_{jns}$$

$$s.t \ \frac{1}{S} \sum_{s=1}^{S} \nu_{ins} \leqslant \alpha_{in} \ \ \forall i \ , \ \mu_{jns} \leqslant \tau_{ij} \left(\frac{w_i}{\varepsilon_{ins}} + \nu_{ins} \right) \ \ \forall i, j, s \ , \ (t_{jns}, \mu_{jns}, 1) \in P_3^{\frac{1}{\sigma}, 1-\frac{1}{\sigma}} \ \ \forall j, s$$

It is easy to see that the objective function is a linear function of t_{jns}*, and that the first and second set of constraints are linear and, thus, convex. It is remaining to show that power conic constraints are also convex.*

Consider $(t^o, \mu^o, 1) \in P_3^{\frac{1}{\sigma}, 1-\frac{1}{\sigma}}$ *and* $(t', \mu', 1) \in P_3^{\frac{1}{\sigma}, 1-\frac{1}{\sigma}}$*, showing that the convexity of these sets amounts to showing that* $(\lambda t^o + (1-\lambda)t', \lambda\mu^o + (1-\lambda)\mu', 1) \in P_3^{\frac{1}{\sigma}, 1-\frac{1}{\sigma}}$*,*

$$\begin{aligned} \lambda t^o + (1-\lambda)t' &\geqslant (\lambda\mu^o)^{1-\sigma} + ((1-\lambda)\mu')^{1-\sigma} \\ &\geqslant \left(\lambda\mu^o + (1-\lambda)\mu'\right)^{1-\sigma} \end{aligned}$$

where the first inequality follows from the definition of power cone and the second inequality from the fact that $f(x) = x^{1-\sigma}$ *is convex for* $x \geqslant 0$. ▫

C.2 Alternative Capacity Cost Functions

Consider the problem outlined in Expression 10 replacing the linear investment cost function with a cost function $f_{in}(C_{in})$ (with the three conditions specified in Subsection 3.3),

$$\max_{C_{in} \geqslant 0} \ \mathbb{E}_{\boldsymbol{\varepsilon_n}} \left[\Pi_n(\boldsymbol{C_n}, \boldsymbol{\varepsilon_n}) \right] - \sum_{i=1}^{I} f_{in}(C_{in}).$$

In this Appendix, I derive the dual for two other specifications of the capacity cost function: a second-degree polynomial, and an exponential function. Then, I provide a solution algorithm for a generic convex investment cost function.

Second-Degree Polynomial: consider the following cost function, $f_{in}(C_{in}) = a_{in}C_{in} + b_{in}C_{in}^2$, with $a_{in}, b_{in} > 0$. The dual of this problem can be written as,

$$\min_{\nu_{ins}, \gamma_{in} \geqslant 0} \frac{\left(\frac{\sigma-1}{\sigma}\right)^{\sigma-1}}{\sigma} \sum_{s=1}^{S} \sum_{j=1}^{J} \frac{\beta_{jn}^{\sigma}}{S} \left(\min_{i} \left\{ \tau_{ij} \left(\frac{w_i}{\varepsilon_{ins}} + \nu_{ins} \right) \right\} \right)^{1-\sigma} + \sum_{i=1}^{I} \frac{\left[\sum_{s=1}^{S} \frac{\nu_{ins}}{S} + \gamma_{in} - a_{in} \right]^2}{4b_{in}}$$

where γ_{in} corresponds to the multiplier on the capacities' non-negativity constraints, and it can be operationalized by noting that the second term corresponds to the power cone:

$$\left(\delta_{in}, 1, \left[\sum_{s=1}^{S} \frac{\nu_{ins}}{S} + \gamma_{in} - a_{in}\right]\right) \in P_3^{\frac{1}{2},\frac{1}{2}}.$$

This allows me to substitute the quadratic term for a linear term, while adding the power cone above as a constraint.

Exponential: consider the following cost function, $f_{in}(C_{in}) = e^{a_{in}C_{in}} - 1$. The dual of this problem is,

$$\min_{\nu_{ins},\gamma_{in}\geqslant 0} \frac{\left(\frac{\sigma-1}{\sigma}\right)^{\sigma-1}}{\sigma} \sum_{s=1}^{S}\sum_{j=1}^{J} \frac{\beta_{jn}^{\sigma}}{S}\left(\min_i\left\{\tau_{ij}\left(\frac{w_i}{\varepsilon_{ins}} + \nu_{ins}\right)\right\}\right)^{1-\sigma} + \sum_{i=1}^{I} \frac{\sum_{s=1}^{S}\frac{\nu_{ins}}{S} + \gamma_{in}}{a_{in}} \times \log\left(\frac{\sum_{s=1}^{S}\frac{\nu_{ins}}{S} + \gamma_{in}}{a_{in}}\right) - \sum_{i=1}^{I} \frac{\sum_{s=1}^{S}\frac{\nu_{ins}}{S} + \gamma_{in}}{a_{in}} + I$$

where γ_{in} corresponds to the multiplier on the capacities' non-negativity constraints. The key to solving this version of the problem consists on realizing that this cost structure adds two terms. The last term is linear, and easy to handle. The other term corresponds to a relative entropy cone $\{(u,v,w) \in \mathbb{R}^{1+2n} : u \geqslant \sum_{i=1}^{n} w_i \log(\frac{w_i}{v_i}), v_i \geqslant 0, w_i \geqslant 0\}$ of dimension $2n+1$ (see Legat et al. 2021). In terms of the expression above, this insight can be used to replace this nonlinear term for a linear term δ, and adding the cone $(\delta, 1, \{\frac{\sum_{s=1}^{S}\frac{\nu_{ins}}{S}+\gamma_{in}}{a_{in}}\}_i)$ as an additional constraint.

General Convex Costs: consider a cost function, $f_{in}(C_{in})$. We solve the problem in two steps. First, notice that regardless of the capacity cost function the dual of the ex-post problem in Equation 7 is,

$$\min_{\nu_{in}\geqslant 0} \sum_{i=1}^{I} \nu_{in}C_{in} + \frac{\left(\frac{\sigma-1}{\sigma}\right)^{\sigma-1}}{\sigma} \sum_{j=1}^{J} \beta_{jn}^{\sigma}\left(\min_i\left\{\tau_{ij}\left(\frac{w_i}{\varepsilon_{in}} + \nu_{in}\right)\right\}\right)^{1-\sigma},$$

and can be written linearly as,

$$\min_{\nu_{in}\geqslant 0,\mu_{jn}>0,t_{jn}>0} \sum_{i=1}^{I} \nu_{in}C_{in} + \frac{\left(\frac{\sigma-1}{\sigma}\right)^{\sigma-1}}{\sigma} \sum_{j=1}^{J} \beta_{jn}^{\sigma} t_{jn}$$
$$\text{s.t } \mu_{jn} \leqslant \tau_{ij}\left(\frac{w_i}{\varepsilon_{in}} + \nu_{in}\right) \quad \forall i,j; \quad (t_{jn}, \mu_{nj}, 1) \in P_3^{\frac{1}{\sigma},1-\frac{1}{\sigma}} \quad \forall j.$$

For a particular vector $\boldsymbol{C_n}$ and $\boldsymbol{\varepsilon_n}$, solving the problem above provides a value the vector of multipliers, $\boldsymbol{\nu_n}(\boldsymbol{C_n}, \boldsymbol{\varepsilon_n})$, and the optimal value of the objective function, $\Pi_n(\boldsymbol{C_n}, \boldsymbol{\varepsilon_n})$.

The *ex-post* problem corresponds to

$$\max_{C_{in} \geqslant 0} \ \mathbb{E}_{\boldsymbol{\varepsilon_n}} \left[\Pi_n(\boldsymbol{C_n}, \boldsymbol{\varepsilon_n}) \right] - \sum_{i=1}^{I} f_{in}(C_{in}).$$

From the envelope theorem, the first order condition for the variable C_{in} is given by

$$\mathbb{E}_{\boldsymbol{\varepsilon_n}} \left[\nu_{in}(\boldsymbol{C_n}, \boldsymbol{\varepsilon_n}) \right] \leqslant f'_{in}(C_{in}),$$

which is a generalization of the gradient in Equation 11. The linearity of the problem implies that finding the solution is sufficiently fast. This allows me to overcome the challenge of computing the high-dimensional expectation by approximating it using simulations.

Precisely, given a vector of capacities $\boldsymbol{C}_n$, I compute expected profits and expected multipliers averaging over $s = 1, \ldots, S$ simulation draws,

$$\mathbb{E}_{\boldsymbol{\varepsilon_n}} \left[\Pi_n(\boldsymbol{C_n}, \boldsymbol{\varepsilon_n}) \right] \approx \frac{1}{S} \sum_{s=1}^{S} \Pi_n(\boldsymbol{C}_n, \boldsymbol{\varepsilon}_n^{\boldsymbol{s}}), \qquad \mathbb{E}_{\boldsymbol{\varepsilon_n}} \left[\nu_{in}(\boldsymbol{C_n}, \boldsymbol{\varepsilon_n}) \right] \approx \frac{1}{S} \sum_{s=1}^{S} \nu_{in}(\boldsymbol{C}_n, \boldsymbol{\varepsilon}_n^{\boldsymbol{s}}).$$

Then, I leverage Proposition 1 to use efficient gradient-based optimizers that exploit the convexity and that the explicit gradients to find the global optimum.

D Additional Results

In Table D.1, I present the results for the estimation of the demand elasticity, σ, and the home market effects, as described in Equations 16 and 17. Columns (1) and (2) correspond to the values used in estimation. Column (1) is the elasticity, σ^M, across models within the same brand which are used to aggregate quantities and prices at the firm-level. Column (2) corresponds to the estimate of the elasticity across firms, relevant for the estimation, where $\hat{\sigma} = 1 + 1.593$. Column (3) shows the results if the estimation is carried with log. quantities rather than log shares. Column (4) shows the results from estimating the elasticity in a single nest, for comparison.

From the regressions estimated in Table D.1, I also retrieve brand fixed effects, $\hat{\gamma}_n$. In Figure D.1, I present the correlation between the retrieved brand-specific demand shifters and the average price for each brand, demonstrating that this measure of quality correlates positively with prices. Also, I show the distribution of these brand shifters by the country of origin of each brand.

Table D.1: Demand Elasticity, Brand Shifters and Home Market Effects

Strategy:		Nested		Single Nest
Nest:	Inner	Outer	Outer	
	(1)	(2)	(3)	(4)
	Log Share	Log Share	Log Q	Log Q
Log Price$_{jm}$	-3.280***			-3.887***
	[0.343]			[0.201]
Log Price$_{jn}$		-1.593***	-2.154***	
		[0.170]	[0.169]	
Home Market		1.068***	1.001***	0.636***
		[0.154]	[0.161]	[0.124]
Observations	4,810	617	617	4,885

Notes: This table shows estimates for Regression Equations 16 and (17). Columns (1) corresponds to the estimation of Equation 16. It contains market-brand-year fixed effects and log prices are instrumented by log tariffs. Columns (2) and (3) correspond to OLS regressions of log shares and log quantities on the market-brand fixed effects recovered in Column (1). Column (4) estimates a regression of log quantities on log prices, with log tariffs as instruments, excluding the market-brand-year fixed effects. All the specifications contain market-year fixed effects. Specifications in columns (2) to (4) also contain fixed effects at the brand-level and a home market effect that is a dummy variable equal to 1 if the brand that produces model m is headquartered in market j, and a brand-level fixed effect. Standard errors clustered at the market-brand level reported in brackets. Significance levels: ***$p < 0.01$, **$p < 0.05$, * $p < 0.1$.

Figure D.1: Brand-Specific Demand Shifters

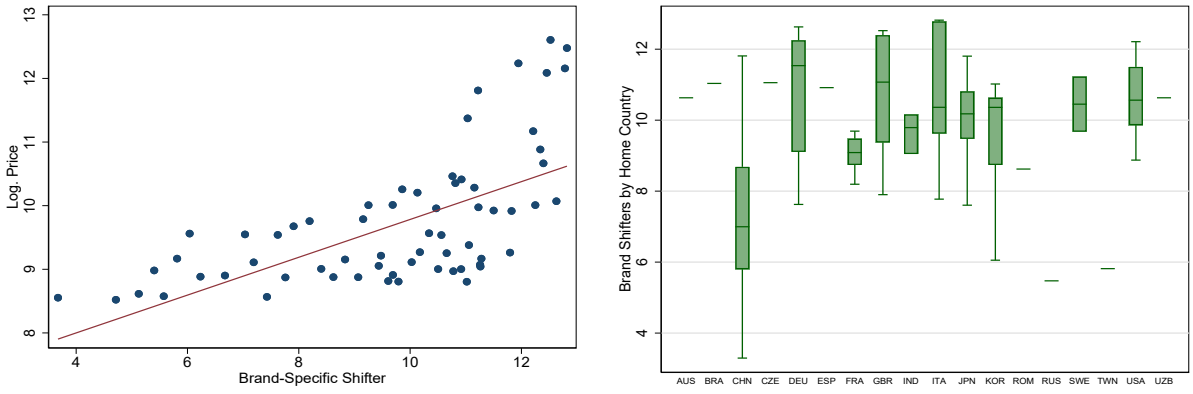

Notes: In Panel (a), I show a binscatter plot between log prices and the brand-specific qualities γ_n computed in the regression in Equation 17. In Panel (b), I show box plots with the distribution of brand qualities by the country of origin of each brand.

In Figure D.2, I present the estimates of the country-specific demand shifters, $\hat{\delta}_j$, as described in Equation 18. These shifters measure aggregate expenditure on cars in market j and the ideal price index at the observed equilibrium.

Figure D.2: Market-Specific Shifters

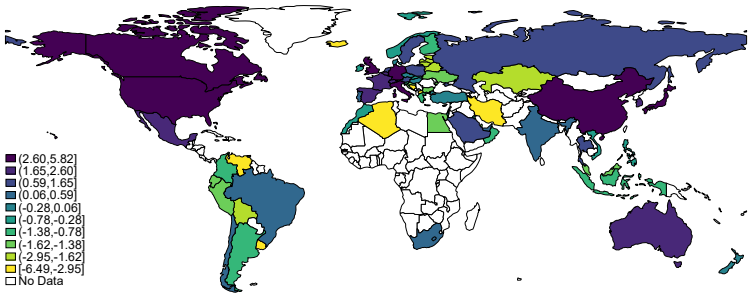

Notes: In this map, I plot the value of the market-specific fixed effects δ_j computed in the regression of Equation 18.

In Table D.2, the values of the estimates of the parameters in the structural model described in Sections 3 and 4. Estimates are computed using the simulated method of moments using the moments described Table E.1. Standard errors are computed using the formula provided in Gourieroux et al. (1993).

Table D.2: Parameter Estimates of the Structural Model

Parameter	Description	Estimate	Standard Error
δ_0^α	Constant - Capacity Cost	3.389	0.001
δ_1^α	Log. Population - Capacity Cost	0.021	0.002
δ_2^α	Log. Road Density - Capacity Cost	0.009	0.001
δ_3^α	Log. GDP Per Capita - Capacity Cost	0.048	0.002
δ_4^α	Home Dummy - Capacity Cost	-0.277	0.001
δ_5^α	Log. Distance HQ - Capacity Cost	0.050	0.002
δ_6^α	Land Availability - Capacity Cost	-0.125	0.001
ξ^α	Variance - Capacity Cost	0.001	0.001
δ_0^ε	Constant - Local Productivity	-3.610	0.002
δ_1^ε	Log. Population - Local Productivity	0.034	0.003
δ_2^ε	Log. Road Density - Local Productivity	0.025	0.003
δ_3^ε	Log. GDP Per Capita - Local Productivity	0.071	0.002
δ_4^ε	Home Dummy - Local Productivity	0.227	0.002
δ_5^ε	Log. Distance HQ - Local Productivity	-0.042	0.003
δ_6^ε	Land Availability - Local Productivity	-0.052	0.002
ξ^ε	Variance - Local Productivity	0.011	0.003
δ_2^w	Wage Shifter - Income Group 2	0.030	0.001
δ_3^w	Wage Shifter - Income Group 3	0.022	0.003
δ_4^w	Wage Shifter - Income Group 4	0.086	0.003
δ_5^w	Wage Shifter - Income Group 5	0.806	0.002
δ_6^w	Wage Shifter - Income Group 6	0.319	0.001
κ_1	Damage 100-Year Flood	0.227	0.005
κ_2	Damage 10-Year Flood	0.415	0.001

Notes: This table shows estimates for the parameters of the structural model introduced in Section 4.2. Estimates computed using SMM with the moments in Table E.1. Model fit is discussed in Appendix Section E.2. Standard errors computed using the formula for simulated method of moments estimators provided in Gourieroux et al. (1993).

Figure D.3: Change in Production Shares for SSP5-8.5

(a) China

(b) United States

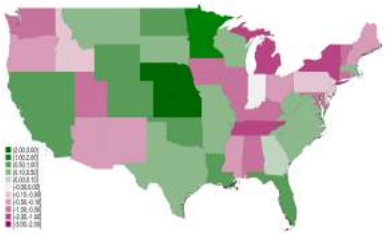

(c) Japan

(d) Germany

(e) India

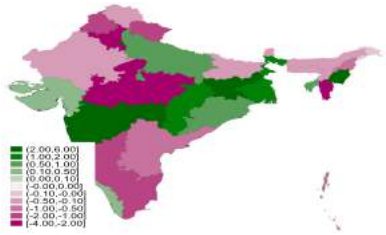

(f) Mexico

(g) South Korea

(h) Brazil

(i) Spain

(j) France

Notes: These maps show changes in production shares (in p.p.) between the current risk landscape, where 10-year floods occur with 10% probability and 100-year floods have a 1% probability, and the projected probabilities for SSP5-8.5. Regions in pink lose production shares, regions in green gain. The estimates used to simulate the model are in Table D.2. The probability projections used come from a multimodel ensemble for SSP5-8.5 from the Climate Change Knowledge Portal of the World Bank. The administrative units in the map correspond to GAUL1 units.

E Estimation

E.1 Moments

Table E.1 shows the moments targeted for the estimation of the parameters in the structural model described in Sections 3 and 4. In describing these moments, I abuse notation as production Y_{in} will be equal to 0 in most places, deeming $\log Y_{in} = \infty$. Instead, I compute the log over the selected sample for which $Y_{in} > 0$. This is harmless as I am applying the same selection criteria in the data and in the model. For each moment, I present the value in the data and in the model, and the squared percentage deviation. The variables $\{\log GDP_i, \log Pop_i, \log Roads_i, Land_i\}$ are demeaned.

Table E.1: Targeted Moments

Description	Data	Model	% Dev. Sq	Description	Data	Model	% Dev. Sq
$\mathbb{E}\left[\sum_{i=1}^{I} \log Y_{in}\right]$	53.60	37.75	0.09	$\mathbb{E}\left[\sum_{i=1}^{I} \log Y_{in} \times 1\{G_i = 3\}\right]$	3.68	2.16	0.17
$\mathbb{E}\left[\sum_{i=1}^{I} \log Y_{in} \times \log GDPPC_i\right]$	-15.36	-13.31	0.02	$\mathbb{E}\left[\sum_{i=1}^{I} \log Y_{in} \times 1\{G_i = 4\}\right]$	4.32	3.24	0.06
$\mathbb{E}\left[\sum_{i=1}^{I} \log Y_{in} \times \log Population_i\right]$	39.07	29.54	0.06	$\mathbb{E}\left[\sum_{i=1}^{I} \log Y_{in} \times 1\{G_i = 5\}\right]$	10.40	4.82	0.29
$\mathbb{E}\left[\sum_{i=1}^{I} \log Y_{in} \times \log RoadDens_i\right]$	6.79	7.88	0.03	$\mathbb{E}\left[\sum_{i=1}^{I} \log Y_{in} \times 1\{G_i = 6\}\right]$	7.18	6.24	0.02
$\mathbb{E}\left[\sum_{i=1}^{I} \log Y_{in} \times \log DistHome_i\right]$	-144.56	-130.36	0.01	$\mathbb{E}\left[\sum_{i=1}^{I} \log Y_{in} \times 1\{G_i = 2\} \times Home_{in}\right]$	9.18	9.02	0.00
$\mathbb{E}\left[\sum_{i=1}^{I} \log Y_{in} \times \log Land_i\right]$	54.61	39.97	0.07	$\mathbb{E}\left[\sum_{i=1}^{I} \log Y_{in} \times 1\{G_i = 3\} \times Home_{in}\right]$	0.08	0.09	0.01
$\mathbb{E}\left[\sum_{i=1}^{I} \log Y_{in} \times Home_{in}\right]$	20.61	18.16	0.01	$\mathbb{E}\left[\sum_{i=1}^{I} \log Y_{in} \times 1\{G_i = 4\} \times Home_{in}\right]$	0.33	0.23	0.08
$\mathbb{E}\left[\sum_{i=1}^{I} D_{in}\right]$	5.26	5.33	0.00	$\mathbb{E}\left[\sum_{i=1}^{I} \log Y_{in} \times 1\{G_i = 5\} \times Home_{in}\right]$	6.58	4.82	0.07
$\mathbb{E}\left[\sum_{i=1}^{I} D_{in} \times \log GDPPC_i\right]$	-1.67	-2.05	0.05	$\mathbb{E}\left[\sum_{i=1}^{I} \log Y_{in} \times 1\{G_i = 6\} \times Home_{in}\right]$	3.74	3.69	0.00
$\mathbb{E}\left[\sum_{i=1}^{I} D_{in} \times \log Population_i\right]$	3.80	3.36	0.01	$\mathbb{E}\left[\sum_{i=1}^{I} D_{in} \times 1\{G_i = 2\}\right]$	2.09	2.29	0.01
$\mathbb{E}\left[\sum_{i=1}^{I} D_{in} \times \log RoadDens_i\right]$	0.63	0.83	0.11	$\mathbb{E}\left[\sum_{i=1}^{I} D_{in} \times 1\{G_i = 3\}\right]$	0.38	0.41	0.00
$\mathbb{E}\left[\sum_{i=1}^{I} D_{in} \times \log DistHome_i\right]$	-13.79	-13.08	0.00	$\mathbb{E}\left[\sum_{i=1}^{I} D_{in} \times 1\{G_i = 4\}\right]$	0.44	0.59	0.11
$\mathbb{E}\left[\sum_{i=1}^{I} D_{in} \times \log Land_i\right]$	5.40	5.70	0.00	$\mathbb{E}\left[\sum_{i=1}^{I} D_{in} \times 1\{G_i = 5\}\right]$	1.01	0.54	0.22
$\mathbb{E}\left[\sum_{i=1}^{I} D_{in} \times Home_{in}\right]$	1.99	1.95	0.00	$\mathbb{E}\left[\sum_{i=1}^{I} D_{in} \times 1\{G_i = 6\}\right]$	0.63	0.67	0.00
$\mathbb{E}\left[\log Y_n^2\right]$	24.35	19.78	0.04	$\mathbb{E}\left[\sum_{i=1}^{I} D_{in} \times 1\{G_i = 2\} \times Home_{in}\right]$	0.94	1.02	0.01
$\mathbb{E}\left[\log D_n^2\right]$	2.16	2.26	0.00	$\mathbb{E}\left[\sum_{i=1}^{I} D_{in} \times 1\{G_i = 3\} \times Home_{in}\right]$	0.01	0.01	0.04
$\mathbb{E}\left[\log Y_n\right]$	4.30	4.04	0.00	$\mathbb{E}\left[\sum_{i=1}^{I} D_{in} \times 1\{G_i = 4\} \times Home_{in}\right]$	0.03	0.03	0.00
$\mathbb{E}\left[\log D_n\right]$	1.03	1.17	0.02	$\mathbb{E}\left[\sum_{i=1}^{I} D_{in} \times 1\{G_i = 5\} \times Home_{in}\right]$	0.63	0.54	0.02
$\mathbb{E}\left[\log Y_n \times \log D_n\right]$	6.45	5.26	0.03	$\mathbb{E}\left[\sum_{i=1}^{I} D_{in} \times 1\{G_i = 6\} \times Home_{in}\right]$	0.32	0.34	0.00
$\mathbb{E}\left[\sum_{i=1}^{I} 1\{\log D_n = 0\}\right]$	0.38	0.22	0.19	$\mathbb{E}\left[\log Y_{in} \times 1\{Max\}\right]$	10.80	10.66	0.00
$\mathbb{E}\left[\sum_{i=1}^{I} 1\{\log D_n < log(3)\}\right]$	0.54	0.45	0.03	$\mathbb{E}\left[\log Y_{in} \times 1\{Max\} - \log Y_{in} \times 1\{2nd\}\right]$	0.71	1.70	1.90
$\mathbb{E}\left[\sum_{i=1}^{I} 1\{\log D_n < log(6)\}\right]$	0.74	0.75	0.00	$\mathbb{E}\left[\sum_{s=1}^{\tilde{S}} \sum_{i=1}^{I} \log Y_{in}^{(s)} \left(\frac{1\{Flood_{in}^{(s)}-1\}}{\sum_{s=1}^{\tilde{S}} 1\{Flood_{in}^{(s)}-1\}} - \frac{1\{Flood_{in}^{(s)}-0\}}{\sum_{s=1}^{\tilde{S}} 1\{Flood_{in}^{(s)}-0\}}\right)\right]$	-0.29	-0.47	0.38
$\mathbb{E}\left[\sum_{i=1}^{I} 1\{\log D_n > log(11)\}\right]$	0.13	0.12	0.00	$\mathbb{E}\left[\sum_{s=1}^{\tilde{S}} \sum_{i=1}^{I} \log Y_{in}^{(s)} \left(\frac{1\{100YFlood_{in}^{(s)}-1\}}{\sum_{s=1}^{\tilde{S}} 1\{100YFlood_{in}^{(s)}-1\}} - \frac{1\{Flood_{in}^{(s)}-0\}}{\sum_{s=1}^{\tilde{S}} 1\{Flood_{in}^{(s)}-0\}}\right)\right]$	-0.50	-0.51	0.00
$\mathbb{E}\left[\sum_{i=1}^{I} \log Y_{in} \times 1\{G_i = 2\}\right]$	21.42	16.92	0.04	$\mathbb{E}\left[\sum_{s=1}^{\tilde{S}} \sum_{i=1}^{I} \log Y_{in}^{(s)} \left(\frac{1\{10YFlood_{in}^{(s)}-1\}}{\sum_{s=1}^{\tilde{S}} 1\{10YFlood_{in}^{(s)}-1\}} - \frac{1\{Flood_{in}^{(s)}-0\}}{\sum_{s=1}^{\tilde{S}} 1\{Flood_{in}^{(s)}-0\}}\right)\right]$	-0.24	-0.42	0.54

E.2 Model Fit

In Table E.1, I show the value of the targeted moments in the data, in the model and the percentage deviation. Overall, the estimation procedure performs reasonably well, matching successfully most of the targeted moments. The model does a good job at matching the moments related to the geographic location of plants, and the features of the distributions of plants and total production at the firm level. However, the procedure struggles with four moments. The worst moment corresponds to the difference in plant production between the first and second largest plants, where the difference implied by the estimates is larger than

the one in the data. Second, the model underestimates both average production and number of plants in countries in the second largest bin of GDP per capita, which includes Belgium, Spain, France, the United Kingdom, Italy, Japan and Korea. However, it is worth noting that I am matching the moments for production and plant location in those countries by local firms. Third, the model is overestimating the impact of 10-year floods on production, although it is matching the impact of 100-year floods closely.

In Figure E.1, I explore the performance of the model in some moments that are not directly targeted. Specifically, I analyze how the model replicates the sales, plant location, and production at the country level, rather than at the smaller geographical units in which the firm decides. The relationship of the sales by country generated by the model and the data is very good, with a high R^2 and intercept close to 0 and a slope coefficient close to 1. Regarding production at the country level, the model does a good job at replicating production in big countries, but yields too little production in small countries.

Figure E.1: Model Fit - Sales and Production by Country

(a) Sales by Country

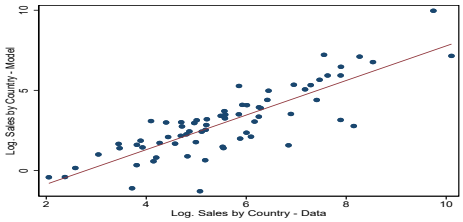

(b) Production by Country

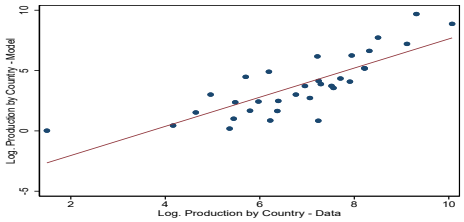

Notes: In Panel (a), I show a binscatter plot for the log of total sales in the model and in the data. In Panel (b), I show a biscatter plot for log of total production in the model and in the data.

Figure E.2 shows that the model produces a geographic distribution of plants that resembles the one in the data as shown in Panel (a), where I show the number of plants per country in the data and in the model as a binscatter plot. In Panel (b), I show the distributions of log production per firm. In Panel (c), I plot a histogram for the distribution of the number of plants. In particular, the model does a good job in matching the number firms with few plants and has a harder time in matching firms in the right tail of the distribution. One implication of replicating this distribution is that the model, matches the number of zeros in the data. In fact, the average firm in the data has 5.26 plants, and in the model 5.33. Clearly, this is not a coincidence since this is an estimation target. Finally, in Panel (d) I show the distribution of plant sizes, as measured by log output per plant, where the model has a harder time in matching the empirical distribution. Basically, the

plant size distribution inherits the Log-Normal shape, that comes from the distributional assumptions I impose over the structural errors. The empirical distribution of plant sizes is somewhat skewed to the left, which is a feature that is challenging to match with Log-Normal distributions that are right-skewed. However, the model does a good job in matching the share of small plants, which is also a moment included in the estimation.

Figure E.2: Model Fit - Distribution of Plants by Firm and on Space

(a) Plants by Country

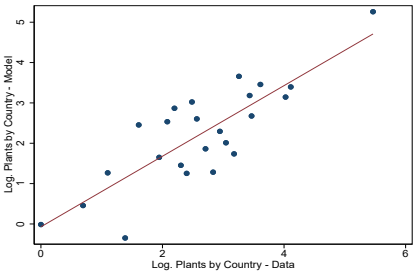

(b) Density of Production by Firm

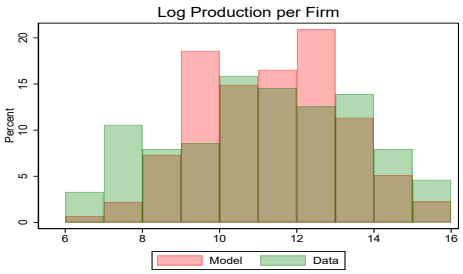

(c) Density of Plants by Firm

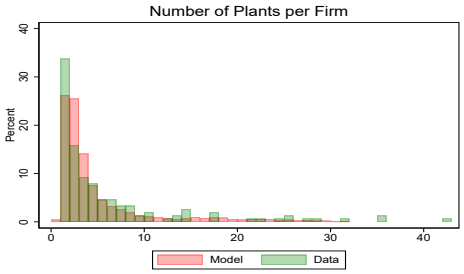

(d) Density of Plant Sizes

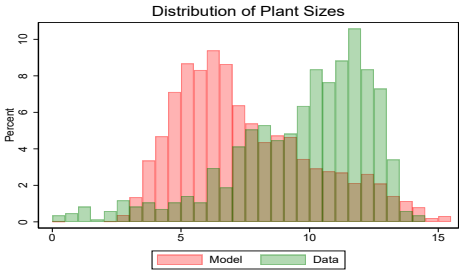

Notes: In Panels (a), I show the number of plants per country in the data and in the model as a binscatter plot. In Panel (b) I show a histogram of the log quantity produced per firm, both in the data and in the model. In Panel (c) I show a histogram of the number of plants per firm, both in the data and in the model. In Panel (d), I show a histogram of plant sizes, as measured by log output per plant, in the data and in the model.

F Additional Counterfactual Exercises

F.1 Spatially Correlated Weather Shocks

An important assumption in the baseline exercise is that the weather shocks are independent across locations. However, in reality, one could expect that regions close to each other are likely to experience spatially correlated shocks, and that firms adjust their plant location taking this positive covariance into account.

I assume that the spatial correlation in the disasters between two locations is a function

of the distance between the centroids of the two administrative units and exponentially decays as locations get farther away. I choose different values for this exponential decay and compare the predictions of the model under different values of the decay.

I generate correlated weather shocks by assuming that these random variables are from a latent spatially-correlated Normal distribution. Let r_i be the probability that κ_i is equal to κ_1 and s_i the probability that κ_i is equal to κ_2 and define $Z_i^1 = \Phi^{-1}(r_i)$ and $Z_i^2 = \Phi^{-1}(s_i)$ and define the following multinomial distribution:

$$\kappa_{in} = \begin{cases} \kappa_1 & \text{if } u_{in}^* \leqslant Z_i^1 \\ \kappa_2 & \text{if } Z_i^1 \leqslant u_{in}^* \leqslant Z_i^2 \\ 1 & \text{if } Z_i^2 \leqslant u_{in}^*, \end{cases}$$

where the u_{in}^* are distributed as the following Multivariate Normal:

$$\boldsymbol{u_n^*} \sim \mathbb{N}(0, \Omega).$$

I assume that the entries of the variance-covariance matrix Ω are given by

$$\Omega_{ii} = 1 \text{ for all } i, \quad \Omega_{ij} = exp(-\lambda dist_{ij}) \text{ for all } i \neq j,$$

where λ measures the decay in the degree of spatial correlation in the latent variable. To illustrate the implied correlations in the weather shocks I pick different values of λ and consider two locations at 300km (1st percentile), 800km (5th percentile) and 1300 km (10th percentile). These are roughly the distances between the centroids of Ohio and Indiana, between Massachusetts and Virginia, and Madrid and Dublin, respectively.

Table F.1: Correlation in Weather Shocks for Different Values of λ

Distance	**300**	**800**	**1300**
$\lambda = 0.02$			
Correlation in Latent Variables	0.549	0.202	0.074
Correlation in Weather Shocks	0.294	0.083	0.027
$\lambda = 0.1$			
Correlation in Latent Variables	0.050	0.000	0.000
Correlation in Weather Shocks	0.018	0.000	0.000

G A Simple Two Location, One Market Model

In this appendix, I present a simplification of the model in Section 3 to study its properties and provide intuition on the identification.

G.1 Analytics

There is a single market, i.e., $J = 1$, and two potential production locations, i.e. $I = 2$. I assume that the market size and the wages in each location are equal to 1, i.e., $\beta = 1, w_1 = 1, w_2 = 1$. To ship goods from each plant to consumers, firms need to pay an homogeneous iceberg cost equal to τ. Only location 1 can experience a weather disruption that is binary and equal to κ with probability p or to 1. The undisrupted production costs in each location are given by z_1 and z_2, assuming $z_1 > z_2 > \kappa z_1$ without loss.

Consider the capacity choice problem for a particular firm with productivity ϕ,

$$\max_{C_1, C_2} \quad (1-p)\Pi\left(C_1, C_2, z_1, z_2\right) + p\Pi\left(C_1, C_2, \kappa z_1, z_2\right) - \alpha\left(C_1 + C_2\right).$$

The *ex-post* profit function is given by

$$\Pi\left(C_1, C_2, \varepsilon_1, \varepsilon_2\right) \equiv \max_{q_1, q_2 \geqslant 0} \quad \left(q_1 + q_2\right)^{\frac{\sigma-1}{\sigma}} - \frac{\tau}{\phi}\left(\frac{q_1}{\varepsilon_1} + \frac{q_2}{\varepsilon_2}\right) \quad \text{s.t} \quad \tau q_1 \leqslant C_1 \quad \forall i \quad [\nu_1], \quad \tau q_2 \leqslant C_2 \quad \forall i \quad [\nu_2].$$

where I denote by ε_1 and ε_2, the realized productivities in each location. For arbitrary values of $C_1, C_2, \varepsilon_1, \varepsilon_2$, and $\varepsilon_1 \geqslant \varepsilon_2$ (again, without loss), *ex-post* profits can take four values,

$$\Pi\left(C_1, C_2, \varepsilon_1, \varepsilon_2\right) = \begin{cases} \left(C_1 + C_2\right)^{\frac{\sigma-1}{\sigma}} \tau^{\frac{1-\sigma}{\sigma}} - \frac{C_1}{\phi\varepsilon_1} - \frac{C_2}{\phi\varepsilon_2} & \text{if} \quad \frac{C_1+C_2}{\tau} < \left(\frac{\sigma-1}{\sigma}\right)^{\sigma} \tau^{-\sigma}\phi^{\sigma}\varepsilon_2^{\sigma} \\ \frac{\left(\frac{\sigma-1}{\sigma}\right)^{\sigma-1}}{\sigma} \tau^{1-\sigma}\left(\phi\varepsilon_2\right)^{\sigma-1} + \frac{C_1}{\phi}\left[\frac{1}{\varepsilon_2} - \frac{1}{\varepsilon_1}\right] & \text{if} \quad \frac{C_1+C_2}{\tau} \geqslant \left(\frac{\sigma-1}{\sigma}\right)^{\sigma} \tau^{-\sigma}\phi^{\sigma}\varepsilon_2^{\sigma} \\ & \text{and} \quad \frac{C_1}{\tau} < \left(\frac{\sigma-1}{\sigma}\right)^{\sigma} \tau^{-\sigma}\phi^{\sigma}\varepsilon_2^{\sigma} \\ \left(C_1\right)^{\frac{\sigma-1}{\sigma}} \tau^{\frac{1-\sigma}{\sigma}} - \frac{C_1}{\phi\varepsilon_1} & \text{if} \quad \frac{C_1}{\tau} < \left(\frac{\sigma-1}{\sigma}\right)^{\sigma} \tau^{-\sigma}\phi^{\sigma}\varepsilon_1^{\sigma} \\ & \text{and} \quad \frac{C_1}{\tau} \geqslant \left(\frac{\sigma-1}{\sigma}\right)^{\sigma} \tau^{-\sigma}\phi^{\sigma}\varepsilon_2^{\sigma} \\ \frac{\left(\frac{\sigma-1}{\sigma}\right)^{\sigma-1}}{\sigma} \tau^{1-\sigma}\left(\phi\varepsilon_1\right)^{\sigma-1} & \text{if} \quad \frac{C_1}{\tau} \geqslant \left(\frac{\sigma-1}{\sigma}\right)^{\sigma} \tau^{-\sigma}\phi^{\sigma}\varepsilon_1^{\sigma}. \end{cases}$$

In the first case, capacity in both plants binds. In the second case, capacity in the most productive plant binds, but in the other plant, it does not, although it is being used. In the third case, capacity in the best plant is binding, and the other plant is unused. In the fourth case, capacity in the most productive plant is not binding. Regardless of the plants' capacities, the firm has incentives to use the most productive plant as much as possible, where the quantity is dictated either by demand and production costs, or by the capacity constraint.

Based on the profit function above, one can compute $\nu_1(C_1, C_2, \varepsilon_1, \varepsilon_2)$ and $\nu_2(C_1, C_2, \varepsilon_1, \varepsilon_2)$ by taking the derivative of the profit function with respect to C_1 and C_2. For example, for C_1 this yields,

$$\nu_1(C_1, C_2, \varepsilon_1, \varepsilon_2) = \begin{cases} \frac{\sigma-1}{\sigma}(C_1+C_2)^{-\frac{1}{\sigma}}\tau^{\frac{1-\sigma}{\sigma}} - \frac{1}{\phi\varepsilon_1} & \text{if } \frac{C_1+C_2}{\tau} < \left(\frac{\sigma-1}{\sigma}\right)^{\sigma}\tau^{-\sigma}\phi^{\sigma}\varepsilon_2^{\sigma} \\ \left[\frac{1}{\varepsilon_2} - \frac{1}{\varepsilon_1}\right] & \text{if } \frac{C_1+C_2}{\tau} \geqslant \left(\frac{\sigma-1}{\sigma}\right)^{\sigma}\tau^{-\sigma}\phi^{\sigma}\varepsilon_2^{\sigma} \\ & \text{and } \frac{C_1}{\tau} < \left(\frac{\sigma-1}{\sigma}\right)^{\sigma}\tau^{-\sigma}\phi^{\sigma}\varepsilon_2^{\sigma} \\ \frac{\sigma-1}{\sigma}(C_1)^{-\frac{1}{\sigma}}\tau^{\frac{1-\sigma}{\sigma}} - \frac{1}{\phi\varepsilon_1} & \text{if } \frac{C_1}{\tau} < \left(\frac{\sigma-1}{\sigma}\right)^{\sigma}\tau^{-\sigma}\phi^{\sigma}\varepsilon_1^{\sigma} \\ & \text{and } \frac{C_1}{\tau} \geqslant \left(\frac{\sigma-1}{\sigma}\right)^{\sigma}\tau^{-\sigma}\phi^{\sigma}\varepsilon_2^{\sigma} \\ 0 & \text{if } \frac{C_1}{\tau} \geqslant \left(\frac{\sigma-1}{\sigma}\right)^{\sigma}\tau^{-\sigma}\phi^{\sigma}\varepsilon_1^{\sigma}, \end{cases}$$

which I plot for both capacities, fixing an arbitrary value for the other, below.

Figure G.1: Ex-Post Multipliers

(a) ν_1 (b) ν_2

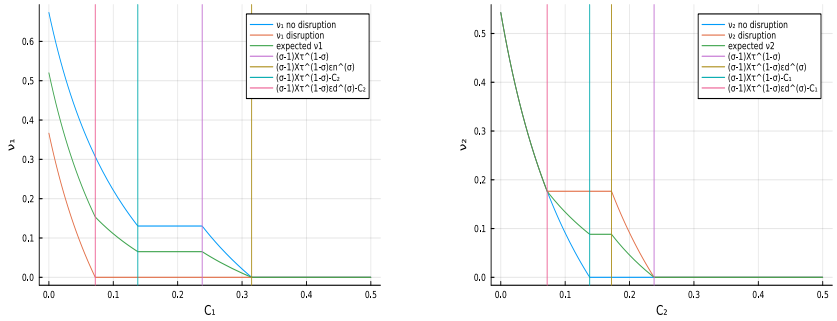

Turning to the capacity choice problem, the first order conditions for the capacity choice problem are, $\mathbb{E}_{\varepsilon_1}[\nu_1(C_1, C_2, \varepsilon_1, \varepsilon_2)] \leqslant \alpha$, $\mathbb{E}_{\varepsilon_1}[\nu_2(C_1, C_2, \varepsilon_1, \varepsilon_2)] \leqslant \alpha$. For instance, if we were to assume that the parameters of the model are such, that it is profitable to only use the plant that is the most productive in each state of the world, the optimal values for capacity investment are:

$$C_1^* = \left(\frac{\alpha}{1-p} + \frac{1}{\phi z_1}\right)^{-\sigma}\left(\frac{\sigma-1}{\sigma}\right)^{\sigma}\tau^{1-\sigma}; \qquad C_2^* = \left(\frac{\alpha}{p} + \frac{1}{\phi z_2}\right)^{-\sigma}\left(\frac{\sigma-1}{\sigma}\right)^{\sigma}\tau^{1-\sigma}$$

Since these assumptions are restrictive, I instead turn to solving the optimal values of capacities numerically for different assumptions on the distribution of shocks. I explore two different instances. First, in Figure G.2, a case in which I hold κ fixed and vary p, and, second, in Figure G.3, a case in which I vary the value of p, and adjust z_1 holding κ fixed in such a way that the mean of the distribution of shocks is held constant $\left(z_1(p) = \frac{1-\kappa p}{1-p}\right)$, but the variance increases, to study the implications of the model for mean preserving spreads.

Figure G.2: Optimal Capacity Investment with Increasing Probabilities

(a) C_1 (b) C_2 (c) Spare Capacity

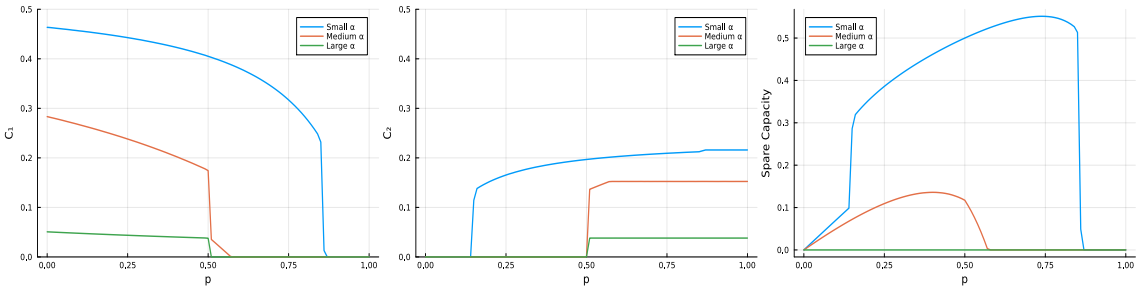

Figure G.3: Optimal Capacity Investment with Mean Preserving Spreads

(a) C_1 (b) C_2 (c) Spare Capacity

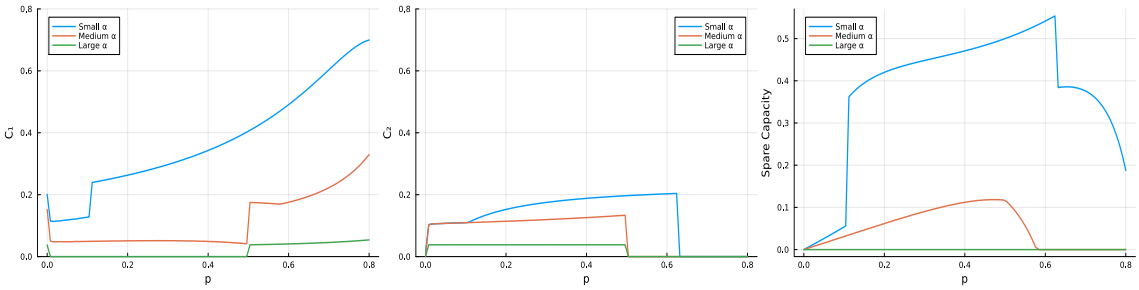

In both cases, I show the optimal values of capacity and the expected spare capacity, varying the value of α as well.

G.2 Identification

Building on the simple example in Subsection G.1, I illustrate how the values of the location parameters of the productivities, z_{1n}, and the capacity costs, α_{in}, are separately identified. I assume that trade costs are homogeneous and equal to $\tau = 1.05$, that the probability of the shock, p, is equal to 0.5, that $\kappa = 0.5$, that $\sigma = 2$ and that $\beta = 1$. Firms are heterogeneous in their productivities ϕ_n. I further assume that both α_{in} and z_{1n} are drawn from these Log-Normal distributions, $\alpha_{in} \sim \bar{\alpha} LogNormal(-1/2, 1)$ and $z_{1n} \sim \bar{z} LogNormal(-1/2, 1)$, respectively. The parameters to identify are $\bar{\alpha}$ and $\bar{z}$.

I define the two following moments, which are the same as the first and the eight moment used for estimation as described in Table E.1,

$$\boldsymbol{m}_1 = \mathbb{E}\left[\frac{1}{2}\sum_{i=1,2} \log Y_{in}\right] \quad \text{and} \quad \boldsymbol{m}_2 = \mathbb{E}\left[\frac{1}{2}\sum_{i=1,2} D_{in}\right].$$

In this setting, I show how the values of the moments $\boldsymbol{m}_1$ and $\boldsymbol{m}_2$ vary with the value of $\bar{\alpha}$ and $\bar{z}$. To analyze this, I simulate the model for 10,000 firms, setting as "true" values, $\bar{\alpha} = 0.25$ and $\bar{z} = 1.25$, and then I compare how the values of moments $\boldsymbol{m}_1$ and $\boldsymbol{m}_2$ corresponding to the "true" model compare to those generated under alternative values by computing the squared percentage deviation. In Figure G.4, I plot in black, combinations

Figure G.4: Impact of $\bar{\alpha}$ and $\bar{z}$ on Moments

(a) $\boldsymbol{m}_1$ (b) $\boldsymbol{m}_2$ (c) $\boldsymbol{m}_1 + \boldsymbol{m}_2$

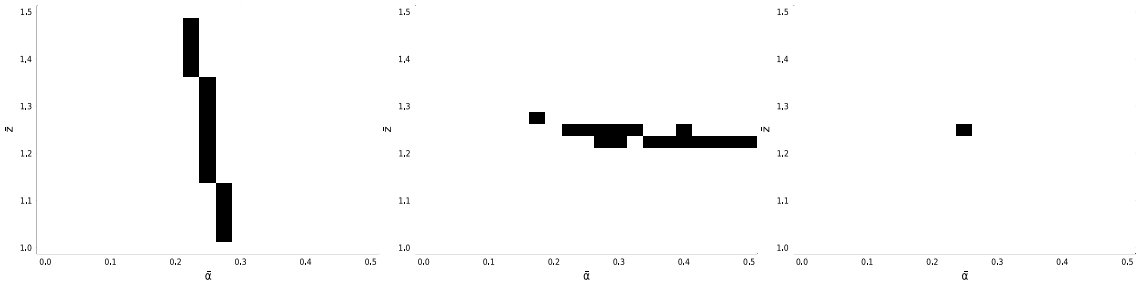

of the values for the parameters $\bar{\alpha}$ and $\bar{z}$ in which the value of the percentage squared deviation between the simulated moment and the "true" data is smaller than 10^{-5}. The figure highlights how moments $\boldsymbol{m}_1$ and $\boldsymbol{m}_2$ jointly identify the parameters of interest. As shown, $\boldsymbol{m}_1$ is a moment that varies mostly with $\bar{\alpha}$. Intuitively, in this context firms are often capacity constrained and the capacity choice is more responsive to changes in its cost. On the contrary, $\boldsymbol{m}_2$ is a moment that varies mostly with $\bar{z}$. Intuitively, in this setting, if either $\bar{z}$ is too high or too low, firms have incentives to concentrate their production in only one plant. Although neither moment alone is individually identifying one of the parameters, once we consider $\boldsymbol{m}_1$ and $\boldsymbol{m}_2$ jointly, there is a single combination of parameters for which the sum of squared percentage deviation is equal to 0.